

# We are IntechOpen, the world's leading publisher of Open Access books Built by scientists, for scientists

6,900

Open access books available

185,000

International authors and editors

200M

Downloads

Our authors are among the

154

Countries delivered to

TOP 1%

most cited scientists

12.2%

Contributors from top 500 universities



WEB OF SCIENCE™

Selection of our books indexed in the Book Citation Index  
in Web of Science™ Core Collection (BKCI)

Interested in publishing with us?  
Contact [book.department@intechopen.com](mailto:book.department@intechopen.com)

Numbers displayed above are based on latest data collected.  
For more information visit [www.intechopen.com](http://www.intechopen.com)



---

# AC Variable-Speed Drives and Noise of Magnetic Origin: A Strategy to Control the PWM Switching Effects

---

Jean-François Brudny, Fabrice Morganti and  
Jean-Philippe Lecoïnte

Additional information is available at the end of the chapter

<http://dx.doi.org/10.5772/64520>

---

## Abstract

The presented developments concern the definition of a method to characterize simply the pulse width-modulated (PWM) switching three-phase harmonic systems. This characterization, which makes it possible to control the components generated by the switching anticipating the negative effects possibly generated, is exploited in the context of reducing the noise of magnetic origin that can affect the operating of AC variable speed drives.

**Keywords:** AC variable speed drives, noise of magnetic origin, radial vibrations, PWM inverters, switching control

---

## 1. Introduction

The use of Pulse Width-Modulated (PWM) inverters is widespread since many years in the field of variable speed AC motor drives. The main advantage, in addition to the offered flexibility and the implementation easiness, concerns the rejection at high frequencies of the voltage switching three-phase harmonic systems (STPHSs). This naturally leads to minimizing their effects considering the inductive machine behavior at these frequencies. The beneficial aspects are real for the torque harmonics [1, 2] insofar as the concerned mechanical resonances, which are characterized by frequencies varying from a few tens to a few hundred Hz, can amplify the effects of low frequency components as, for example, six-step inverters. However, other phenomena, particularly important, may occur. The latter concern the iron [3, 4] and copper losses, the noise of magnetic origin [5, 6] but also premature aging of the electrical

---

winding insulation [7, 8]. To overcome these effects, a simple solution consists of introducing a filter connected to the inverter outputs. However, taking into account the additional costs required by this solution that also increases the size of the “inverter,” this technique is not always compatible with the industrial constraints. That is why research teams have proposed other solutions to control some of these effects. These last can be grouped into three categories. The first acts on the power electronic converter architecture in order to minimize the voltage variation amplitude during a switching leading, for example, to the multilevel converters [9]. The second concerns the machine design [10], by introducing, for example, specific dampers [11, 12] to reduce the switching air gap flux density harmonics. The third concerns the definition of specific control strategies.

The study presented in this chapter is in the third category, with the goals of reducing the noise of magnetic origin. Many references dealing with this particular subject appear in the scientific literature [13–18]. Realized developments present the originality to remove a force component whose effects are particularly troublesome if that component excites a stator mechanical resonance that may be located at frequencies of a few kHz which correspond, in terms of human hearing response, to a particularly sensitive area [19]. Let us assume that this force component is generated by a given balanced STPHS in the output signals of the converter. The principle consists in removing this STPHS by making homopolar an intermediate STPHS which is at its origin. This principle, which requires to use three distinct carriers, has been already presented [20–22]. It is based primarily on the STPHS phase angle determination. To facilitate this determination, a Sinus–Sinus (SS) PWM is associated to the classic Sinus–Triangle ( $S\Delta$ ) PWM. It has also been shown that this suppression has a drawback insofar it is accompanied by the appearance of certain harmonics, which are in some cases unbalanced, that may challenge the proposed principle. To minimize the negative effects of this procedure, a strategy called “carrier-phase jump” [22] is presented, it consists of removing alternately two STPHSs from the output signals, exploiting the additional degree of freedom provided by this technique. Then, a procedure that uses carriers defined with different frequencies is disclosed.

This chapter is therefore mainly devoted to the presentation and the experimental implementation of the methods just mentioned, considering a symmetrical, “p” pole pair induction machine (IM) whose magnetic circuit is supposed to be nonsaturated. The used inverter has a basic structure: two levels and triangular carriers. As the inverter generates voltage STPHSs, some of them being unbalanced, the first part concerns the characterization of the acoustic noise generated by the IM in these conditions. Such an analysis seems a priori original as the state-of-the-art shows that no study have been proposed with such an approach. The second part shows the method to characterize simply the STPHSs, especially their harmonic-phase sequences. The third part presents the application of the method and the control strategy applied to the inverter in order to act on STPHSs. The possible negative effects of the control are also described. In order to minimize these effects, the fourth part exposes the carrier-phase jump control that has not been published in a journal. The fifth part presents, for the first time, the method that consists in using different frequencies for the three carriers. The last part is devoted to the presentation of experimental results concerning IM magnetic noise and radial vibration reductions.

A time “k” rank harmonic of a variable “z” on phase “q” (q = 1, 2 or 3) will be denoted  $z_q^k$ . Let us point out that upper indexes “(s)” and “(Δ)” will also be used to distinguish the variables according to the sinusoidal or triangular carrier waveforms. No index means that the relations are valuable whatever the case. The STPHSs will be characterized not only by their frequency but also with the order of the phase sequence: Clockwise (C), Anticlockwise (A), and Homopolar (H).

## 2. Magnetic noise components

The presentation of the proposed strategy requires to fully understand the origins of the various force components that produce the mechanical deformations of the stator massive external housing. This justifies the developments that are presented in this section. They are based on the definition of the “b” air gap flux density harmonic content. As saturation is neglected, “b” is substantially independent of the IM load conditions and, consequently, is defined by the product [23, 24]:

$$b = \varepsilon \Lambda \tag{1}$$

$\varepsilon$  is the air gap magnetic potential difference generated by the stator at no load and  $\Lambda$  models the air gap per unit area permanence. The power supply fundamental frequency is denoted by “f” (angular frequency  $\omega$ , period T). Regarding  $\Lambda$ , the relationship established in Ref. [25] is used:

$$\Lambda = \sum_{k_s} \sum_{k_r} \Lambda_{k_s k_r} = \sum_{k_s} \sum_{k_r} \hat{\Lambda}_{k_s k_r} \cos[(k_s N^s + k_r N^r) \alpha - k_r N^r \mathcal{D}] \tag{2}$$

$N^s$  and  $N^r$  define the stator and rotor saliency numbers (teeth).  $k_s$  and  $k_r$  are integers varying from  $-\infty$  to  $+\infty$ . Let us consider a  $d^s$  stator spatial reference that is assumed to be confounded with the Phase 1 axis.  $\alpha$  makes it possible to locate any point of the air gap with respect to  $d^s$  and  $\mathcal{D}$  characterizes the rotor position relative to the same reference. Assuming that the rotor speed is imposed by (C) fundamental three-phase voltage system, it can be written:  $\mathcal{D} = (1-s)\theta/p + \mathcal{D}_0$ , with “s” the IM slip,  $\theta = \omega t$  and  $\mathcal{D}_0$  the  $\mathcal{D}$  value for  $t = 0$ . A wave with a positive direction of rotation will be considered in the trigonometric direction, like the fundamental wave. A negative direction characterizes a wave rotating in the opposite direction. The permanence expression given by the relationship (2) is composed of:

- a constant term  $\Lambda_{00}$  which characterizes the air gap corrected thickness used to design the IMs,
- terms which depend on the stator toothings  $\Lambda_{k_s 0}$ ,

- terms which depend on the rotor tothing  $\Lambda_{0k_r}$ ,
- terms  $\Lambda_{k_s k_r}$  (for  $k_s$  and  $k_r \neq 0$ ), which model the interaction between stator and rotor toothings.

In order to fix the approximated values of the terms, depending on the tothing, it can be noted that  $\Lambda_{k_s 0}$ ,  $\Lambda_{0k_r}$  and  $\Lambda_{k_s k_r}$  are, respectively, inversely proportional to  $|k_s|$ ,  $|k_r|$  and  $|k_s k_r|$ .

The expression (2), in its formulation, is similar to expressions given by other authors. Alger [23] considers the same relation but with only the fundamental of each group of terms ( $k_s = k_r = 1$ ). Timar [24] considers the harmonic components with  $\Lambda_{k_s 0}$  and  $\Lambda_{0k_r}$  but neglects the terms  $\Lambda_{k_s k_r}$  by arguing that their contribution is low, which is erroneous when the slotting resonance phenomenon appears [25].

## 2.1 Case of balanced STPHSs

Assuming that (H) systems do not exist in the  $v_q$  voltages applied to the stator windings, “k” can be defined as a positive or negative integer that characterizes (C) and (A), respectively, balanced systems so that:

$$\varepsilon = \sum_k \sum_h \varepsilon_h^k = \sum_k \sum_h \hat{\varepsilon}_h^k \cos[k\theta - hp\alpha - \phi_h^k] \quad (3)$$

“h” defined by:  $h = 1 + 6n$  with “n” an integer varying from  $-\infty$  to  $+\infty$ , defines the rank of the space harmonics related to the nonuniform distribution of the winding wires at the stator frame.  $\alpha$  is an angular abscissa for positioning any point of the air gap with respect to  $d^s$ . Let us point out that  $\hat{\varepsilon}_h^k$  is inversely proportional to “h” and also to “k” because the RMS values of the  $i_q^k$  currents which define  $\hat{\varepsilon}_h^k$  decrease generally with “k”.

It follows that “b” is expressed by:

$$b = \sum_k \sum_h \sum_{k_s} \sum_{k_r} b_{hk_s k_r}^k \quad (4)$$

This “b” relationship leads to the “F” Maxwell force per unit area acting on the stator inner frame. Noting  $\mu_0$  the air permeability ( $\mu_0 \approx 4\pi 10^{-7} H/m$ ), “F” is defined by:

$$F = \frac{1}{2\mu_0} \left[ \sum_k \sum_h \sum_{k_s} \sum_{k_r} b_{hk_s k_r}^k \right]^2 \quad (5)$$

leading to express, in general [22], “F” by:

$$F = \sum_K \sum_H \sum_{K_s} \sum_{K_r} \hat{F}_{HK_s K_r}^K \cos[\Pi_{K_r}^k \theta - P_{HK_s K_r} \alpha + \varphi_{HK_r}^K] \quad (6)$$

These force components are very numerous, but all of them do not generate magnetic noise. In fact, the components to be considered must be characterized by:

- a  $\hat{F}_{HK_s K_r}^K$  sufficient amplitude,
- a relatively small  $P_{HK_s K_r}$  mode number ( $P_{HK_s K_r} < 8$ ),
- a frequency  $\Pi_{K_r}^k f$  close to a stator frame natural frequency.

As the sums imply several variables, it is obvious that the analytical expressions of the force components become heavy. As a result, to make the study easier, the phase angles will not be considered so that the characteristics will concern the frequencies and the pole numbers of the force components. Moreover, the components will be selected by taking into account only the forces which may have sufficient amplitudes. This approach allows taking into account the fact that the model given by Eq. (2) for characterizing the tothing, relies on hypotheses that decrease the reliability of the determination concerning the flux density components, and thus the force components, of very low amplitudes.

This approach is so justified in view of the criteria which characterize an annoying force. Indeed, it is shown that a force of high amplitude may have any effect on the noise although a force component with a much lower amplitude can be particularly important in terms of noise if its frequency is close to a natural resonance of the stator stack. However, at this level of the study, another difficulty concerns the transfer function for calculating the radial vibration amplitudes due to the force components. Analytical expressions have been proposed [23, 26], but the models are relatively inaccurate; the error on the vibration amplitudes, and so on the noise, may be important. The explained considerations reinforce our approach to characterize “F”; it consists in not systematically calculating the formal value of the amplitudes. In these conditions, introducing the following quantities:

$$\left. \begin{aligned} S &= N^r(1-s)/p \\ hp_{(+)} &= hp + (k_s N^s + k_r N^r) \\ hp_{(-)} &= hp - (k_s N^s + k_r N^r) \\ \hat{b}_{hk_s k_r}^k &= \hat{\varepsilon}_h^k \hat{\Lambda}_{k_s k_r} / 2 \end{aligned} \right\} \quad (7)$$

It can be written:

$$b_{hk_s k_r}^k = \hat{b}_{hk_s k_r}^k \left\{ \cos[(k - k_r)S\omega t - hp_{(-)}\alpha] + \cos[(k + k_r)S\omega t - hp_{(+)}\alpha] \right\} \quad (8)$$

The component selection is done from the development of the square of expression (8), considering the previous criteria about the force amplitudes. Considering expression (5), it appears that some force terms result from the square of each flux density term, the others force components depending on the double products between the flux density components. The numerical calculations [25] show, considering the fundamental component, that  $\hat{b}_{100}^1 > > \hat{b}_{hk_s k_r}^1$  for every combination “ $hk_s k_r$ ” different from “100”. For example, for a classical machine, for  $\hat{b}_{100}^1 = 1T$ ,  $\hat{b}_{hk_s k_r}^1$  is about 0.02 T for the highest values which correspond to the first values of the parameters that intervene in the inferior combination. It means that concerning the squared terms, only  $(\hat{b}_{100}^1)^2$  has to be considered because, for a combination inferior different from “100,” the other squared terms leads to terms of which amplitudes, in the most favorable case, are of the order of  $10^4$  lower than  $(\hat{b}_{100}^1)^2$ . Concerning the double products, the previous example shows that only the terms which include  $\hat{b}_{100}^1$  have to be considered.

By extending this particularity to the terms which concern harmonics of “ $k$ ” rank, it appears that “ $F$ ” given by expression (5) can also be written as:

$$F^* = \frac{1}{2\mu_0} \sum_k \sum_h \sum_{k_s} \sum_{k_r} b_{100}^k b_{h'k'_s k'_r}^{k'} \quad (9)$$

The use of  $F^*$  instead of  $F$  distinguishes the force defined by the rules of art or according to our agreement to simplify the mathematical developments with an impact mainly on the “ $F$ ” component amplitudes.

Introducing the parameters  $k'$ ,  $h'$ ,  $k'_r$  and  $k'_s$ , that have the same functionality as  $k$ ,  $h$ ,  $k_s$  and  $k_r$ , makes it possible to distinguish two terms, generally different, to exploit the sums defined

by expressions (4) and (5). On the other hand, if for a “k” given value,  $k'$ ,  $h'$ ,  $k'_r$  and  $k'_s$  take all the values in their variation domain, the expression (9) takes also into account the force components which result from the squared terms. Thus, to characterize “ $F^*$ ,” a relationship similar to expression (6) will be used, by adapting the coefficients of expression (6). It can be written:

$$F^* = \sum_k \sum_{h'} \sum_{k'_s} \sum_{k'_r} F_{h'k'_sk'_r}^{k,k'} = \sum_k \sum_{h'} \sum_{k'_s} \sum_{k'_r} \hat{F}_{h'k'_sk'_r}^{k,k'} \cos[\Pi_{h'k'_sk'_r}^{k,k'} \theta - P_{h'k'_sk'_r}^{k,k'} \alpha] \quad (10)$$

The use of (9) allows to do a systematic sum without any analysis but with the drawback of a high uncertainty concerning the amplitudes. However, this uncertainty is not of importance insofar a selection of the component was made and, on the other hand, this uncertainty may be of the same order as the fact to neglect the phase angles. In return, the analytical expressions are notably simplified, but with a strict respect of the frequencies and the pole numbers. Developing the product  $b_{100}^k b_{h'k'_sk'_r}^{k'}$  leads to show that  $F_{h'k'_sk'_r}^{k,k'}$  is composed of four terms whose coefficients  $\Pi_{h'k'_sk'_r}^{k,k'}$  and  $P_{h'k'_sk'_r}^{k,k'}$  are given in **Table 1**. Their exploitation requires to consider first the upper signs and then the lower ones.

	$\Pi_{h'k'_sk'_r}^{k,k'}$	$P_{h'k'_sk'_r}^{k,k'}$	$\Pi_{h'k'_sk'_r}^{k,k'}$	$P_{h'k'_sk'_r}^{k,k'}$
$b_{100}^k b_{h'k'_sk'_r}^{k'}$	$k + k' \mp k'_r S$	$p + h' p_{(\mp)}$	$k - k' \pm k'_r S$	$p - h' p_{(\mp)}$

**Table 1.** Characterization of the  $b_{100}^k b_{h'k'_sk'_r}^{k'}$  coefficients.

At this stage of our developments, two cases may be considered according to the “k” values.

Let us consider the relationship:  $v_q^k = \frac{d\psi_q^k}{dt}$ , where  $\psi_q^k$  corresponds to phase “q” linked flux resulting from air gap magnetic effects generated by the “k” rank three-phase harmonic voltage. It can be shown, for given “f,” that  $\hat{b}_{100}^k$  is proportional to  $\hat{v}_q^k$  and inversely proportional to “k”. Let us assume that  $\hat{v}_q^k$  is same order of magnitude as  $\hat{v}_q^1$ .

- For low “k” values (first odd values),  $\hat{b}_{100}^k$ , for  $k \neq 1$ , is practically the same order of magnitude as  $\hat{b}_{100}^1$ . This means that the relation (10) should be used as presented.

- For high “k” values such as those that characterize STPHSs,  $\hat{b}_{100}^k$ , for  $k \neq 1$ , is very small comparing  $\hat{b}_{100}^1$ . For example, considering the case of a supply via a PWM inverter, for a switching frequency of 50 times greater than “f,” the largest amplitude of these harmonic components, considering the previous equality on the voltages, is in the range of 0.02 T for  $\hat{b}_{100}^1 = 1T$ . Given the comments that were made earlier about the amplitudes of the components resulting from the slotting effect, it can be deduced that the squared amplitudes of flux density components generated by the switching, for the most important, are of the order of  $10^4$  lower than  $(\hat{b}_{100}^1)^2$ . Therefore, the effects of teeth associated with these quantities may be neglected. Then, Eq. (9) can be written as follows:

$$F^* = \frac{1}{2\mu_0} \left\{ \sum_h \sum_{k_s} \sum_{k_r} b_{100}^1 b_{hk_s k_r}^{1'} + \sum_k b_{100}^k b_{100}^{k'} \right\} \tag{11}$$

leading to define  $F^*$  by the relationship:

$$F^* = \sum_h \sum_{k_s} \sum_{k_r} \hat{F}_{hk_s k_r}^{1,1} \cos[\Pi_{hk_s k_r}^{1,1'} \theta - P_{hk_s k_r}^{1,1'} \alpha] + \sum_k \sum_{k_r} \hat{F}_{100}^{k,k'} \cos[\Pi_{100}^{k,k'} \theta - P_{100}^{k,k'} \alpha] \tag{12}$$

whose coefficients are given in **Table 2**.

	$\Pi_{hk_s k_r}^{k,k'}$	$P_{hk_s k_r}^{k,k'}$	$\Pi_{hk_s k_r}^{k,k'}$	$P_{hk_s k_r}^{k,k'}$
$\hat{b}_{100}^1 \hat{b}_{hk_s k_r}^1$	$2 \mp k_r S$	$p + hp_{(\mp)}$	$\pm k_r S$	$p - hp_{(\mp)}$
$\hat{b}_{100}^k \hat{b}_{100}^{k'}$	$k+k'$	$2p$	$k-k'$	$0$

**Table 2.** Characterization of the coefficients which define  $F^*$  for high “k” values.

Considering Eq. (10), the square of the rank “k” term is obtained for  $k = k'$  by considering the inferior combination “100” for “h’, k’, k’”. This also corresponds, considering Eq. (12), to exploit the coefficients of the second row of **Table 2** with  $k' = k$ . It results that these squares lead to two force components which can be identified with  $\hat{F}_{100}^{k,k} \cos[2k\theta - 2p\alpha]$  and  $\hat{F}_{100}^{k,k}$ . The first term is a rotating wave with a speed  $k\omega/p$  and with a direction positive or negative according to the sign of “k”. The second term leads to a permanent deformation of the IM external housing with a constant amplitude. This force component does not generate any vibration and so any noise. It is qualified as stationary force.

## 2.2. Case of unbalanced STPHSs

It is supposed that, even for this case, there is no (H) systems that is justified in section III. In order to distinguish, for a “k” given value, the kf frequency (C) and (A) systems that appear with the imbalance, the ranks  $k_C$  and  $k_A$  are introduced. Previously, this distinction was not necessary insofar as harmonic phase system was either (C) or (A), implicitly, “k” so take either the value  $k_C$  or  $k_A$ . In this case, for certain values of “k,”  $\varepsilon_h^k$  is expressed as follows:

$$\varepsilon_h^k = \hat{\varepsilon}_h^{k_C} \cos[k_C\theta - hp\alpha] + \hat{\varepsilon}_h^{k_A} \cos[k_A\theta - hp\alpha] \quad (13)$$

The single goal of introducing  $k_C$  and  $k_A$  is to distinguish the systems knowing that the absolute values of  $k$ ,  $k_C$  and  $k_A$  are equal, but the amplitudes of the components relative to  $k_C$  and  $k_A$  are generally different. If, before the imbalance, “k” was positive, then  $k_C$  is positive and  $k_A$  is negative. If, on the contrary, before the imbalance “k” was negative, then  $k_C < 0$  and  $k_A > 0$ . As the definition of “h” is not changed, it appears that, for  $h > 0$  and  $k < 0$ , the mmf component depending on  $k_A$  corresponds in fact to a (C) system.

The relationship (9) does not change, only the set of possible values of “k” is enriched following the splitting of certain harmonic three-phase systems. It follows that  $F^*$  is still given by Eqs. (10) or (12) so that **Tables 1** and **2** remain valid. Let us point out finally that the expression (8) that gives  $b_{hk_s k_r}^k$ , assuming that the rank “k” three-phase system is affected by an imbalance, as:  $k = k_C = -k_A$ , becomes:

$$b_{hk_s k_r}^k = b_{hk_s k_r}^{k_C} + b_{hk_s k_r}^{k_A} = \hat{b}_{hk_s k_r}^{k_C} \left\{ \cos[(k - k_r S)\omega t - hp_{(-)}\alpha] + \cos[(k + k_r S)\omega t - hp_{(+)}\alpha] \right\} + \hat{b}_{hk_s k_r}^{k_A} \left\{ \cos[(k + k_r S)\omega t + hp_{(-)}\alpha] + \cos[(k - k_r S)\omega t + hp_{(+)}\alpha] \right\} \quad (14)$$

The force components which result from  $(\hat{b}_{100}^k)^2$ ,  $\hat{b}_{100}^k$  being deduced from Eq. (14), lead to a denser harmonic content compared to the balanced STPHS case. It is composed of:

- a term of the form “ $\cos(2k\omega t - 2p\alpha)$ ” whose amplitude is proportional to  $(\hat{b}_{100}^{k_C})^2$
- a term of the form “ $\cos(2k\omega t + 2p\alpha)$ ” whose amplitude is proportional to  $(\hat{b}_{100}^{k_A})^2$
- a term of the form “ $\cos 2k\omega t$ ” whose amplitude is proportional to the products  $\hat{b}_{100}^{k_C} \hat{b}_{100}^{k_A}$

- two stationary terms whose amplitudes are proportional to  $(\hat{b}_{100}^k)^2$  and to  $(\hat{b}_{100}^k)^2$ ,
- two “pseudo-stationary” terms of the form “ $\cos 2pa$ ” whose amplitudes are proportional to  $\hat{b}_{100}^k \hat{b}_{100}^k$ .

The pseudo-stationary state differs from the stationary state by the fact that the deformation of the stator housing, independent of the time, is nonuniform. Such components do not generate acoustic noise as the stationary components.

The  $\cos 2k\omega t$  terms characterize force components with any pole. Thus the deformation of the external housing is uniform with an amplitude varying with time. This kind of deformation is qualifying of “breathing mode”. Numerical applications will show the acoustic impact of such a force.

Concerning these developments, simplified expressions to characterize the force components in terms of frequencies and polarities, by eliminating components that exhibited too low amplitudes to cause significant effects, have been suggested. However, in terms of simplification, considerations about the pole numbers of the forces can significantly reduce the number of terms to be considered to characterize “F\*”. For example, it is immediately apparent, when  $k_s$  and  $k_r$  are nonzero and of the same sign, the absolute values of the sums which characterize the pole numbers given by (7) are very high and do not comply, therefore, the conditions for retaining the corresponding force components. This will be developed in the next section in relation to numerical applications that concern a three-phase IM with  $p = 2$ ,  $N^S = 36$ , and  $N^r = 24$ .

## 2.3. Numerical applications

### 2.3.1. Practical evaluation of force components

- Assuming that all the STPHSs are balanced, for “ $h$ ” successively equals to 1, -5, 7, -11, 13, -17, 19, -23, and 25, and  $k_s$  and  $k_r$  varying between -9 and +9, the number of force components which have mode numbers lower than 8 has been determined from Eq. (7). This analysis shows that all these components are characterized by  $hp_{(+)} = hp_{(-)} = p = 2$ . Whatever “ $h$ ,” for a given value of  $k_s$ , two force components appear. They are characterized by different values of  $k_r$ , except for  $h = 1$  for which these two values of  $k_r$  are the same leading, because of the particularity concerning the pole numbers, to identical expressions. The number of components to consider according to the values taken by “ $h$ ” is presented in **Table 3**.
- The second criterion concerns the amplitudes by considering  $|hk_s k_r|$  and the terms for which these quantities are lower than 100. Practically, as for the fundamental this quantity is identified to 1, by supposing in first approximation that the force amplitudes are inversely

h	1	-5	7	-11	13	-17	19	-23	25
Criteria: force pole numbers	14	12	12	12	12	14	14	12	12
+ Criteria on the amplitudes	14	8	8	6	6	4	4	4	4

**Table 3.** Numbers of force components for given k and k'.

proportional to  $|hk_s k_r|$  (it is a very optimistic consideration for the amplitudes), it means that the components whose amplitudes are lower than one hundredth of the fundamental amplitude are neglected. When  $|h|$  increases, the number of components, which satisfy the two conditions, decreases. The second row in **Table 3** gives the state of remaining components.

- For given values of  $k$  and  $k'$ , because of the particularity of the force pole numbers, as the frequencies depend only on  $k_r$  as shown in **Table 1**, it is possible to group all the terms with the same  $k_r$ . That way, only 15 distinct components appear as shown in **Figure 1** with gives the theoretical spectrum. The latter shows, the amplitude variations with  $k_r$ . These amplitudes are defined by  $1/|hk_s k_r|$  by taking into account, for each value of  $k_r$ , only the combination defined for the lowest value of  $|hk_s k_r|$ . It can be noted that no component exist for  $k_r = \pm 8$  and  $\pm 7$ . At last, it appears that, for the considered case, the number of components is relatively small while covering rather a wide spectrum. For  $k = k' = 1$  (machine supplied with sinusoidal waves), the frequencies deduced from **Table 1** are given by  $(1 \mp k_r S)f$ . At no load, for  $f = 50$  Hz, the “s” slip is 0.2%, then  $S = 11.976$ . As a result, the spectrum is spread over a frequency band between 0 and 5439 Hz. Assuming, as above, a switching frequency equal to  $50 f$ , the noise components caused by the teeth for the voltage component at 50 Hz will interfere with the noise generated by switching around 2500 Hz and, to a lesser extent, around 5000 Hz. For higher frequencies, only the effects generated by STPHSs will be visible.

### 2.3.2. Impact of an imbalance on the noise measurements

The main practical problem results from nonstationary force components which come from the squares of the terms following the imbalance. Let us denote “B” and “U” quantities contained in Eq. (12) which correspond, respectively, for balanced and unbalanced system. They are representative, to a constant, of the force components which act on the inner periphery of the stator.

$$\left. \begin{aligned} B &= (\hat{b}_{100}^k)^2 \cos(2k\omega t - 2p\alpha) \\ U &= (\hat{b}_{100}^{k_c})^2 \cos(2k\omega t - 2p\alpha) + (\hat{b}_{100}^{k_A})^2 \cos(2k\omega t + 2p\alpha) + \hat{b}_{100}^{k_c} \hat{b}_{100}^{k_A} \cos 2k\omega t \end{aligned} \right\} \quad (15)$$

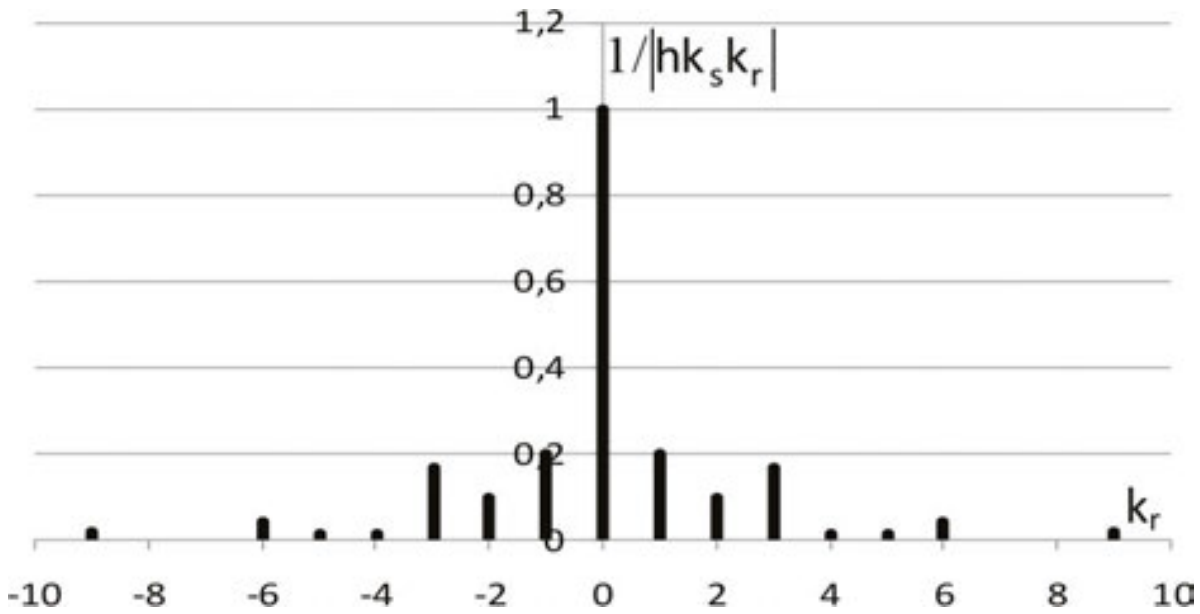


Figure 1. Theoretical frequency components generated by the slotting effect.

As “k” only affects the wave speeds, **Figure 2** presents for  $k = 1$  and  $\alpha$  taking successively the values  $0, \pi/4$  et  $\pi/3$ rd, the variations with time of  $B$  (**Figure 2b**) for  $\hat{b}_{100}^k = 1T$  and of  $U$  (**Figure 2c**) for  $\hat{b}_{100}^{kC} = 0.55T$  and  $\hat{b}_{100}^{kA} = 0.45T$ .

One can note, whatever the position of a microphone or an accelerometer around the IM, the same effects are measured when the STPHS is balanced. When the STPHS is unbalanced, for some positions ( $\alpha = \pi/3$ rd for example), there is practically no effect while at other places ( $\alpha = 0$ rd, for example) these effects are particularly significant.

That is why it is necessary to do measurements with at least two devices spatially shifted to adequately characterize the effects, the shifting being dependent on the wave deformation mode numbers.

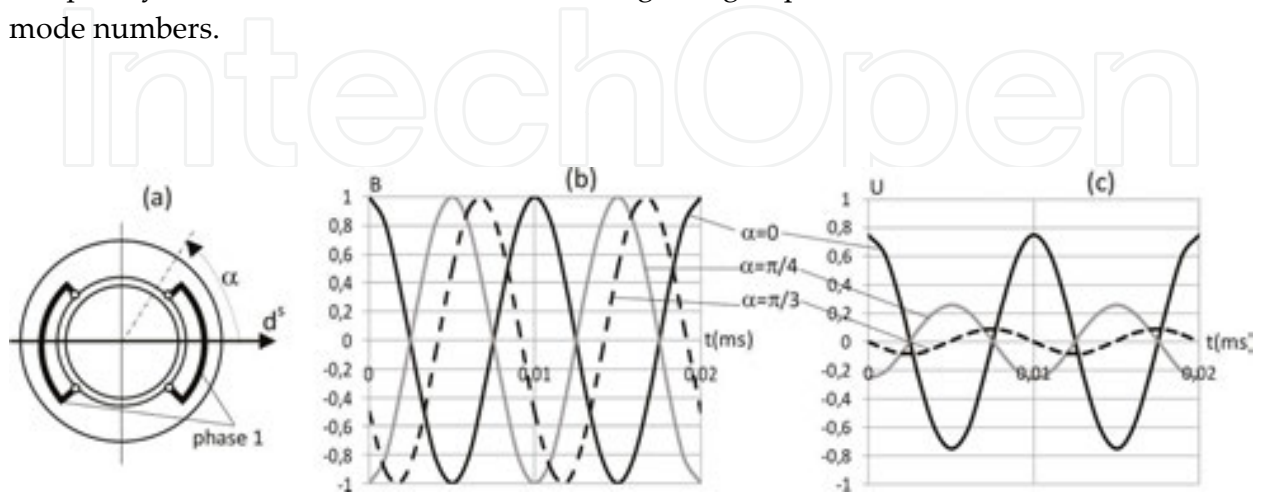
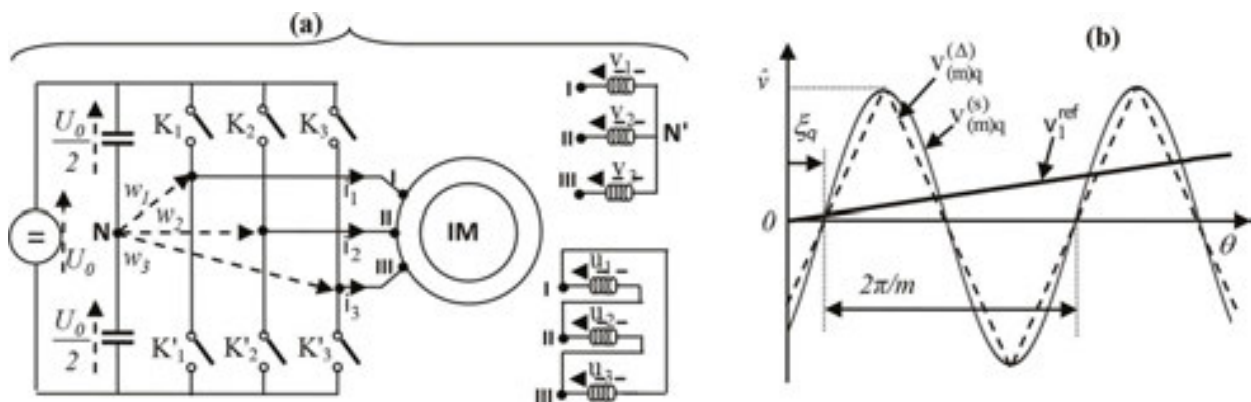


Figure 2. Forces acting on the inner stator surface: (b) balanced STPHS, (c) unbalanced STPHS.

### 3. Voltage supply modeling

Modeling three-phase voltage signals to be applied to the AC machine windings is the subject of the third section which exploits the structure shown in **Figure 3a** characterized by the relationship:

$$\sum_q i_q = 0 \quad (16)$$



**Figure 3.** (a) IM connected to a three-phase PWM inverter, (b) control signals.

Two three-phase voltage systems appear in **Figure 3a**: that of  $v_q$  voltages and that of  $w_q$  voltages still qualified three-phase intermediate voltage system.

#### 3.1. Characterization of the voltage STPHSs applied to the load

Let us consider an unbalanced  $w_q^k$  STPHS of rank “k”. It can be assumed that this  $w_q^k$  system results from the sum of (C), (A), and (H) three-phase elementary systems:

$$w_q^k = w_q^{kC} + w_q^{kA} + w_q^{kH} \quad (17)$$

- For star connected windings (**Figure 3a**), the voltages satisfy the following relationship:

$$w_q = v_q + v_{N'N} \quad (18)$$

which must also be valid pour each harmonic system.

- Consequently, for (C) and (A) systems, one can write:

$$\sum_q w_q^{k_{CorA}} = \sum_q v_q^{k_{CorA}} + 3v_{N'N}^{k_{CorA}} \quad (19)$$

As  $\sum_q w_q^{k_{CorA}} = 0$ , taking into account Eq. (16), leads to:  $\sum_q v_q^{k_{CorA}} = 0$ , so that  $v_{N'N}^{k_{CorA}} = 0$ . It

results in the following equality:  $v_q^{k_{CorA}} = w_q^{k_{CorA}}$ .

- For (H) systems,  $i_q^{k_H}$  currents cannot exist according to Eq. (16). It results that  $v_q^{k_H} = 0$ . As  $w_q^{k_H} = w^{k_H}$  what may be "q," leads to the following equality:  $w_q^{k_H} = v_{N'N}^{k_H}$ . Thus, the potential of N' varies similarly as the (H) components present in the  $w_q$  system avoiding to impact the  $v_q$  system with these (H) components.

- For delta connected windings (**Figure 3a**),  $u_q$  is given par the relationship:  $u_q = w_q - w_{q+1}$ . It appears immediately that  $u_q$  system consists only in (C) and (A) three-phase harmonic systems.

These elementary considerations show that the stator windings, either they are star or delta connected, are not affected by the presence of (H) STPHSs present in the  $w_q$  three-phase system, whereas (C) and (A) STPHSs are fully reflected to the machine input terminals. That property has been used to lead the analysis done in the previous section about the force components. That is also this property which will be used to cancel some harmonic components existing in the machine supply. However, it is required to find easily the phase order sequence of the different  $w_q$  (or  $v_q$ ) STPHSs. That is why a method is then proposed for this determination by considering the equivalent star connected load.

### 3.2. Modeling of the STPHSs

Therefore, an annoying force component generated by the switching can simply be removed by making (H) the  $w_q$  STPHS that is at its origin. It is at this level that the feature of the proposed strategy requires controlling the inverter using a three-phase carrier system. Let us denote  $v_q^{ref}$  and  $v_{(m)q}^{(\Delta)}$  the phase "q" sinusoidal reference and triangular carrier signals, whose angular frequencies are, respectively, " $\omega$ " and  $m\omega$  (frequency  $f_{PWM} = mf$ ). "m" is defined as the modulation index. To characterize analytically the  $w_q$  STPHS phase sequences, since triangular carriers leads to tedious calculations, the authors intend to make these determinations by substituting  $v_{(m)q}^{(s)}$  sinusoidal carriers to  $v_{(m)q}^{(\Delta)}$  triangular carriers, these two signals presenting the same peak values as shown in **Figure 3b**. Let us note that for a classical ( $S\Delta$ ) PWM,  $v_{(m)q}^{(\Delta)}$  is the same whatever "q".

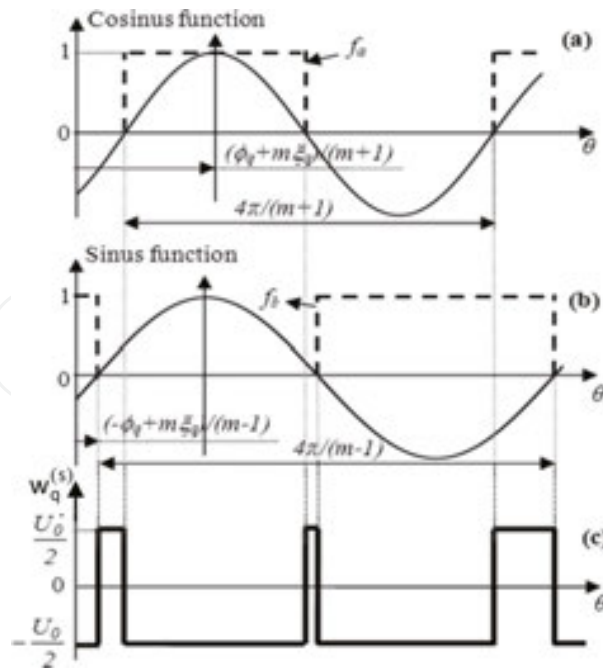


**Figure 4.** Principle of the  $w_q^{(s)}$  determination.

Considering that the “r” adjusting coefficient is equal to the unit and a time referential tied to  $v_1^{ref}$ , introducing  $\phi_q = (q - 1)2\pi/3$ ,  $v_q^{ref}$  and  $v_{(m)q}^{(s)}$  are expressed as:

$$\left. \begin{aligned} v_q^{ref} &= \hat{v} \sin(\theta - \phi_q) \\ v_{(m)q}^{(s)} &= \hat{v} \sin[m(\theta - \xi_q)] \end{aligned} \right\} \quad (20)$$

$\xi_q$  is a phase “q” adjustable carrier phase difference.

- The control strategy is similar to that defined for a (SΔ) PWM: when  $v_q^{ref} > v_{(m)q}^{(s)}$  the  $K_q$  switch is closed and  $w_q^{(s)} = U_0/2$ ; for  $v_q^{ref} < v_{(m)q}^{(s)}$   $K'_q$  is closed and  $w_q^{(s)} = -U_0/2$ . The inequality  $v_q^{ref} > v_{(m)q}^{(s)}$  taking into account Eq. (20) can be written as follows:

$$\cos\left\{\frac{(m+1)\theta - \phi_q - m\xi_q}{2}\right\} \sin\left\{\frac{(m-1)\theta + \phi_q - m\xi_q}{2}\right\} \leq 0 \quad (21)$$

Let us introduce the  $f_a$  and  $f_b$  logic functions defined as:

- $f_a = 1$  or 0 if the cosine is positive or negative, respectively.
- $f_b = 1$  or 0 if the sine is negative or positive, respectively.

It makes it possible to express the  $w_q^{(s)}$  as:

$$w_q^{(s)} = U_0 (2f_a f_b - f_a - f_b + 1/2) \tag{22}$$

Figure 4 shows the principle applied to determine  $w_q^{(s)}$ .

The  $f_a$  and  $f_b$  Fourier series can be written as:

$$\left. \begin{aligned} f_a &= \frac{1}{2} + \frac{2}{\pi} \sum_{n_1=0}^{\infty} \frac{(-1)^{n_1}}{2n_1 + 1} \cos \left\{ \frac{2n_1 + 1}{2} [(m + 1)\theta - \phi_q - m\xi_q] \right\} \\ f_b &= \frac{1}{2} + \frac{2}{\pi} \sum_{n_2=0}^{\infty} \frac{-1}{2n_2 + 1} \sin \left\{ \frac{2n_2 + 1}{2} [(m - 1)\theta + \phi_q - m\xi_q] \right\} \end{aligned} \right\} \tag{23}$$

where  $n_1$  and  $n_2$  are positive or null integers.  $w_q^{(s)}$  can be expressed as:

$$w_q^{(s)} = \sum_{n_1=0}^{\infty} \sum_{n_2=0}^{\infty} (w_q^{(s)k_1} - w_q^{(s)k_2}) \tag{24}$$

where:

$$\left. \begin{aligned} w_q^{(s)k_1} &= \hat{w}^{(s)k_1} \sin (k_1\theta - N^-\phi_q - mN^+\xi_q) \\ w_q^{(s)k_2} &= \hat{w}^{(s)k_2} \sin (k_2\theta - N^+\phi_q - mN^-\xi_q) \end{aligned} \right\} \tag{25}$$

$$\left. \begin{aligned} N^+ &= 1 + n_1 + n_2 \\ N^- &= n_1 - n_2 \end{aligned} \right\} \tag{26}$$

$$\left. \begin{aligned} k_1 &= mN^+ + N^- \\ k_2 &= mN^- + N^+ \end{aligned} \right\} \tag{27}$$

Let us denote  $W_0^{(s)} = 4U_0/\pi^2$ . The component amplitudes that intervene in Eq. (25) are given by  $(1)^{(1+n_1)} W_0^{(s)} / [(2n_1 + 1)(2n_2 + 1)]$ . If  $k_1$  is a positive integer,  $k_2$  can be positive or negative.

To avoid use of negative frequencies but, also, of negative amplitudes, the relationships given by Eq. (25) will be rewritten as:

$$\left. \begin{aligned} w_q^{(s)k_1} &= \hat{w}^{(s)k_1} \sin \left( |k_1| \theta - N^- \phi_q - mN^+ \xi_q - (1+n_1)\pi \right) \\ w_q^{(s)k_2} &= \hat{w}^{(s)k_2} \sin \left( |k_2| \theta - N^+ \phi_q - mN^- \xi_q - n_1\pi \right) \text{ for } k_2 > 0 \\ w_q^{(s)k_2} &= \hat{w}^{(s)k_2} \sin \left( |k_2| \theta + N^+ \phi_q + mN^- \xi_q - (1+n_1)\pi \right) \text{ for } k_2 < 0 \end{aligned} \right\} \quad (28)$$

where

$$\hat{w}^{(s)k_1 \text{ or } k_2} = W_0^{(s)} / \left[ (2n_1 + 1)(2n_2 + 1) \right] \quad (29)$$

k	$n_2 \downarrow n_1 \rightarrow 0$	1	2	3	4	5	
(a): $ k_1 $	0	m; (H); 1	2m + 1; (C); 3	3m + 2; (A); 5	4m + 3; (H); 7	5m + 4; (C); 9	6m + 5; (A); 11
	1	2m - 1; (A); 3	3m; (H); 9	4m + 1, (C); 15	5m + 2; (A); 21	6m + 3; (H); 27	7m + 4; (C); 33
	2	3m - 2; (C); 5	4m - 1; (A); 15	5m; (H); 25	6m + 1; (C); 35	7m + 2; (A); 45	8m + 3; (H); 55
	3	4m - 3; (H); 7	5m - 2; (C); 21	6m - 1; (A); 35	7m; (H); 49	8m + 1; (C); 63	9m + 2; (A); 77
	4	5m - 4; (A); 9	6m - 3; (H); 27	7m - 2; (C); 45	8m - 1; (A); 63	9m; (H); 81	10m + 1; (C); 91
	5	6m - 5; (C); 11	7m - 4; (A); 33	8m - 3; (H); 55	9m - 2; (C); 77	10m - 1; (A); 99	11m; (H); 121
(b): $ k_2 $	0	1; (C)	m + 2; (A)	2m + 3; (H)	3m + 4; (C)	4m + 5; (A)	5m + 6; (H)
	1	m - 2; (C)	3; (H)	m + 4; (C)	2m + 5; (A)	3m + 6; (H)	4m + 7; (C)
	2	2m - 3; (H)	m - 4; (A)	5; (A)	m + 6; (H)	2m + 7; (C)	3m + 8; (A)
	3	3m - 4; (A)	2m - 5; (C)	m - 6; (H)	7; (C)	m + 8; (A)	2m + 9; (H)
	4	4m - 5; (C)	3m - 6; (H)	2m - 7; (A)	m - 8; (C)	9; (H)	m + 10; (C)
	5	5m - 6; (H)	4m - 7; (A)	3m - 8; (C)	2m - 9; (H)	m - 10; (A)	11; (A)

**Table 4.** Characterization of  $w_q^{(s)}$  STPHs generated by the (SS) PWM.

**Table 4** presents, for the first  $n_1$  and  $n_2$  values, the characteristics of the STPHSs of ranks  $|k_1|$  (a) and  $|k_2|$  (b). Information given in **Table 4** concerns the rank of the harmonic and the phase sequence. Concerning  $|k_1|$ , the numerical values of  $\left[ (2n_1 + 1)(2n_2 + 1) \right]$  are also given. As  $1/\left[ (2n_1 + 1)(2n_2 + 1) \right]$  decreases very quickly when  $n_1$  and  $n_2$  increase, the analysis may cover only the first  $n_1$  and  $n_2$  values.

The main conclusion which can be extracted from **Table 4** is that a harmonic of rank “ $k$ ” belongs only to the group  $k_1$  or only to the group  $k_2$ . Furthermore, the rank of this harmonic appears only one time. As a result, considering the expression (28) to characterize the STPHSs, Eq. (24) can be rewritten as:

$$w_q^{(s)} = \sum_k w_q^{(s)k} = \sum_{k_1} w_q^{(s)k_1} - \sum_{k_2} w_q^{(s)k_2} \quad (30)$$

One can note first that these developments are valid whatever the (SS) PWM is, i.e., synchronous or asynchronous. Then, they show that, in this case, STPHSs are either balanced or Homopolar. Consequently, only (C) or (A) STPHSs constitute the  $v_q^{(s)}$  three-phase system according to the study presented in Section 2.1. The fundamental value is obtained from the group  $k_2$  for  $n_1 = n_2 = 0$  and its amplitude is  $W_0^{(s)}$ .

It appears that this analytical model has considerable advantages because it makes it possible to determine the  $w_q^{(s)}$  (or  $v_q^{(s)}$ ) spectral contents and the harmonic phase sequences, without calculating the switching instants.

The problem now is to analyze under what conditions these results are applicable for a (SΔ) PWM and how the “ $r$ ” value impacts on this property established for  $r = 1$ . The developments will be done considering a synchronous PWM.

### 3.3. PWM modeling validation

Let us point out that, from a practical point of view, the  $w_q$  three-phase system is not accessible. Therefore, the validation concerns the  $v_q$  spectral content for sinusoidal  $v_q^{ref}$ ,  $m = 55$ ,  $f = 50\text{Hz}$ ,  $U_0 = 520\text{V}$  and a single carrier wave, by comparing analytical, numerical, and experimental results for  $r = 1$ , then for  $r \neq 1$ .

All the experiments are made by connecting to the inverter outputs a three-phase, 50 Hz, 15 kW, two pole pair cage IM star connected operating at no load. A Focusrite sound card programmed with the C sound language makes it possible to control the switching generating single (or multiple) carrier(s) with sinusoidal (or triangular) shape(s). The  $v_q$  spectral content, both in amplitude and phase, is obtained using a spectrum analyzer. Numerical values come from FFT made with Matlab™ or using a computer program that exploits the calculated switching instants. Cross spectra of  $v_1^k$  and  $v_2^k$  give the phase differences for the main components ( $\delta\hat{v}_q^k > 3\%$ ) so that they define their (C) or (A) phase sequences. Let us point out that  $2\pi/3$  and  $4\pi/3$  differences correspond, respectively, to a (C) and (A) systems.

The  $v_q$  spectral component relative amplitudes defined as percentage result from the relationship:

$$\delta \hat{v}_q^k = 100 \hat{v}_q^k / \hat{v}_q^1 \quad (31)$$

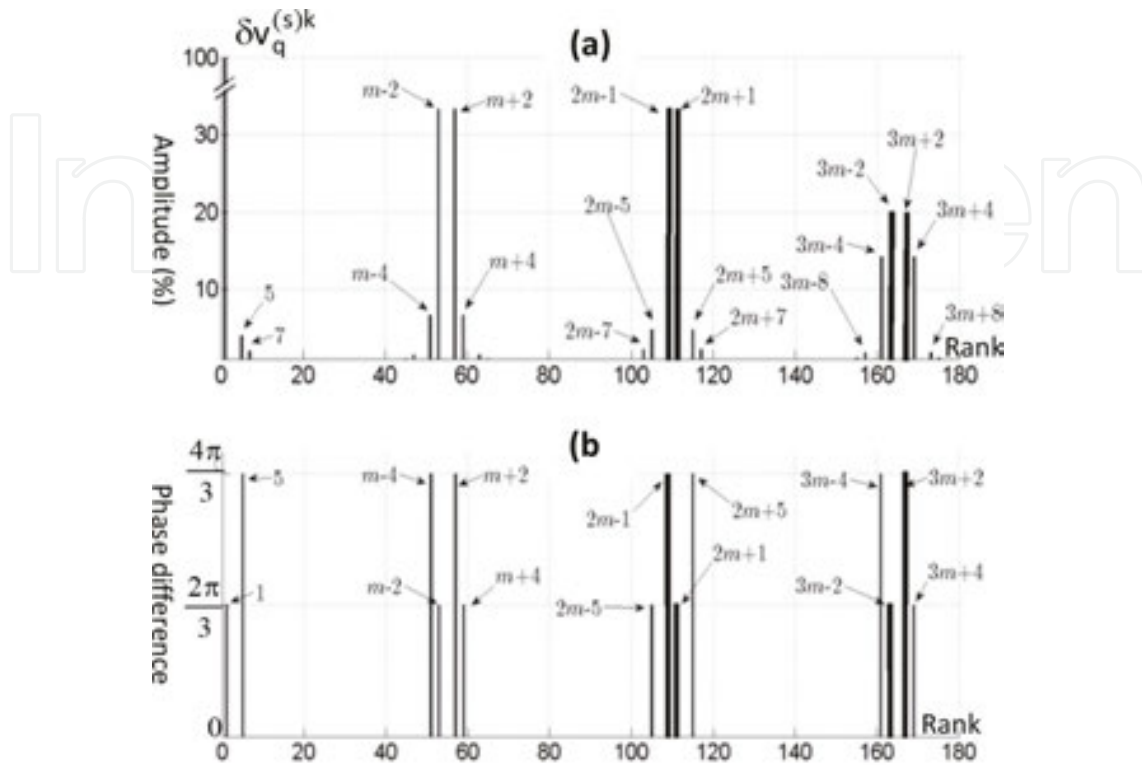


**Figure 5.** Experimental  $v_q^{(s)}$  harmonic content for single sinusoidal carrier,  $m = 55$ ,  $r = 1$  and  $\xi_q = 0$ : (a) Harmonic content (b) phase differences.

### 3.3.1. Single sinusoidal carrier

- For  $r = 1$ ,  $w_q^{(s)}$  analytical harmonic ranks and phase sequences are given in **Table 4** for the first  $n_1$  and  $n_2$  values. As  $\hat{w}_q^{(s)1} = W_0^{(s)}$  where  $W_0^{(s)} = 210.75V$ ,  $\delta \hat{w}_q^{(s)k}$  values are obtained multiplying by one hundred the reversed numerical values given in **Table 4a**.

The  $v_q^{(s)}$  characteristics obtained experimentally for  $\xi_q = 0$  are given in **Figure 5**, where the bold lines correspond to the terms resulting from the  $k_1$  group (deduced from the analytical study). It appears that the number of components from the  $k_1$  group is very limited and that these components appear only in the harmonic families centered on terms multiple of "m".

Analytical and experimental results are in excellent correlation that validates the proposed methodology.

- The characteristics of the main STPHSs have been calculated for different  $\xi_q$  and  $r$  values.

- For  $r = 1$ , whatever the values of  $\xi_{q'}$ , the previous relative amplitudes are found. For the phases, the analytical and numerical values, for given value of  $\xi_{q'}$ , are almost the same, the gap increasing with “m”. For example, for the  $3m + 4$  rank component, the gap is inferior to  $1^\circ$  with the FFT and it is reduced when the switching instants are calculated.

-  $r \neq 1$  leads to a similar spectral content than that is obtained for  $r = 1$  with differences on the spectrum component amplitudes (the reference value in Eq. (31) is the fundamental component magnitude obtained experimentally for the considered “r” value). This analysis leads to a notable result which concerns the phases, and therefore the phase sequences, which are the same that for  $r = 1 \forall r$ .

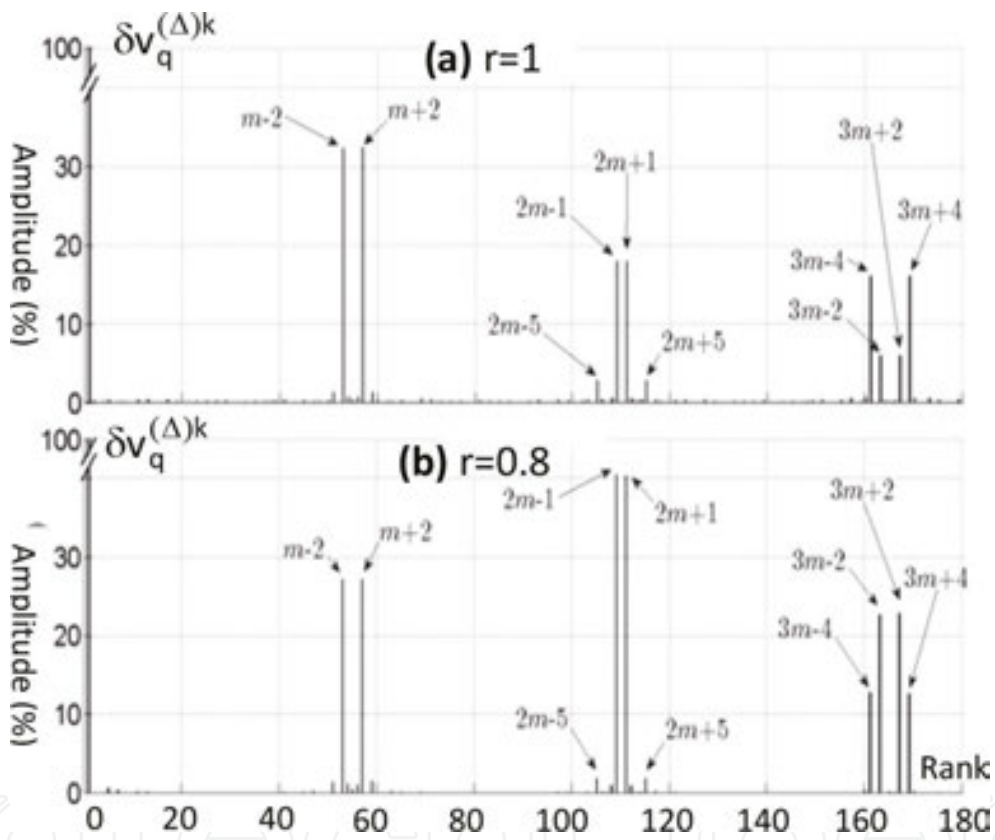


Figure 6. Experimental  $v_q^{(\Delta)k}$  harmonic content for single triangular carrier  $m = 55$ , and  $\xi_q = 0$ : (a)  $r = 1$ , (b)  $r = 0.8$ .

### 3.3.2. Single triangular carrier

Figure 6 shows the experimental  $v_q^{(\Delta)k}$  spectra obtained for  $r = 1$  (Figure 6a) and  $r = 0.8$  (Figure 6b). Eq. (31) makes it possible to calculate  $\delta \hat{w}_q^{(\Delta)k}$  taking into account that  $\hat{v}_q^{(\Delta)1} = rU_0/2$  (260 V for the considered  $U_0$  value and  $r = 1$ ). Comparing Figures 5a and 6a, it appears, independently of the magnitude differences on the fundamental components according to the carrier type, that the same harmonic ranks are practically obtained. For components of low ranks (5 and 7),

the magnitudes are notably amplified with the (SS) PWM, although these components do not intervene predominantly on the spectral content. One can also note that there is an inversion concerning the components of highest amplitude around  $3m$ .

The results obtained on the STPHS phase sequences highlight that they are independent not only from the carrier type but also from the “ $r$ ” and  $\xi_q$  values. Consequently, they can be always deduced from Eq. (28). This property can be expressed as follows: the phase angles calculated with the expression established for a (SS) PWM, thus for  $r = 1$ , are also valuable for the harmonic components, which appears for a (S $\Delta$ ) PWM and this, whatever the value of “ $r$ ”. The fact that “ $r$ ” does not intervene appears in reference [27]. Compared to other methods [28], the one proposed by the authors allows simplifying the PWM analytical expressions which characterize its operating, thanks to the use of logical functions. For example, it has the advantage of not using a Fourier series with Bessel functions, as for the double-Fourier series methods used in reference [29].

The drawback of the proposed method is that it cannot be used if precise determination of the voltage harmonic component amplitudes is required. In fact, concerning this study, this drawback is not really a problem as it is in accordance with the manner of characterizing the force components.

This analysis allows concluding in general about the STPHSs. Indeed, whatever the method (analytical, modeling, or experimentation), the STPHSs satisfy,  $\forall r$ , the following equalities:

$$\left. \begin{array}{l} v_q^k = w_q^k \text{ for (C) and (A) systems} \\ v_q^k = 0 \text{ for (H) systems} \end{array} \right\} \quad (32)$$

#### 4. Simple voltage harmonic control

In this case, the method to simply remove a  $v_q^{(s)}$  STPHS is presented denoting “ $x$ ” or “ $y$ ” the rank of the suppressed STPHS. As, in certain cases, that method leads to generate unbalances on the phases, the voltages will be characterized using “ $q$ ”. As a result, the new STPHSs will be characterized by the variables  $w_{q(xory)}^{(s)k}$  or  $v_{q(xory)}^{(s)k}$  that are sinusoidal functions, which will be defined to a constant that will be denoted, respectively,  $C_{(x)}$  and  $C_{(y)}$ . To illustrate this method, first, two harmonics of the  $k_2$  group, which contributes mainly on the definition of the spectral content, are concerned. Then, two harmonics of the  $k_1$  group will be considered. From a practical point of view, all the results concern (S $\Delta$ ) PWM with  $m = 55$  and  $r = 1$ . The presentation of  $v_q^{(\Delta)}$  spectra used to characterize the various components of a continuous line for (C) systems and a dotted line for (A) systems.

## 4.1. Suppression of $k_2$ group harmonics

### 4.1.1. Principle of the $x = m + 2$ or $y = m - 2$ rank harmonic elimination

- The case of the  $x=m+2$  rank harmonic. As  $k_2 > 0$  with  $n_1 = 1$  and  $n_2 = 0$ , Eq. (28) leads to:

$w_q^{(s)k_2} = \hat{w}^{(s)k_2} \sin\left[|k_2|\theta + \phi_q - m\xi_q - \pi\right]$ . To make this system (H), the condition (33) must be satisfied:

$$m\xi_{q(x)} = \phi_q - C_{(x)} \quad (33)$$

Thus the modified systems, deduced from Eq. (28) can be expressed as:

$$\left. \begin{aligned} w_{q(x)}^{(s)k_1} &= \hat{w}^{(s)k_1} \sin\left[|k_1|\theta - (1 + 2n_1)\phi_q + N^+C_{(x)} - (1 + n_1)\pi\right] \\ w_{q(x)}^{(s)k_2} &= \hat{w}^{(s)k_2} \sin\left[|k_2|\theta - (1 + 2n_1)\phi_q + N^-C_{(x)} - n_1\pi\right] \text{ for } k_2 > 0 \\ w_{q(x)}^{(s)k_2} &= \hat{w}^{(s)k_2} \sin\left[|k_2|\theta + (1 + 2n_1)\phi_q - N^-C_{(x)} - (1 + n_1)\pi\right] \text{ for } k_2 < 0 \end{aligned} \right\} \quad (34)$$

The case of  $y = m - 2$  rank harmonic. The method to suppress the  $v_q^S$ ,  $y = m - 2$  harmonic rank of the  $k_2$  group with  $k_2 < 0$  is similar to the previous one. This harmonic is defined by  $n_1 = 0$  and  $n_2 = 1$ , Eq. (28) leads to  $w_q^{(s)k_2} = \hat{w}^{(s)k_2} \sin\left[|k_2|\theta - \phi_q - m\xi_q - \pi\right]$ . To make this harmonic system (H), it suffices to satisfy the equality in Eq. (35):

$$m\xi_{q(y)} = -\phi_q + C_{(y)} \quad (35)$$

That leads to characterize the modified system by Eq. (36):

$$\left. \begin{aligned} w_{q(y)}^{(s)k_1} &= \hat{w}^{(s)k_1} \sin\left[|k_1|\theta + (1 + 2n_2)\phi_q - N^+C_{(y)} - (1 + n_1)\pi\right] \\ w_{q(y)}^{(s)k_2} &= \hat{w}^{(s)k_2} \sin\left[|k_2|\theta - (1 + 2n_2)\phi_q - N^-C_{(y)} - n_1\pi\right] \text{ for } k_2 > 0 \\ w_{q(y)}^{(s)k_2} &= \hat{w}^{(s)k_2} \sin\left[|k_2|\theta + (1 + 2n_2)\phi_q + N^-C_{(y)} - (1 + n_1)\pi\right] \text{ for } k_2 < 0 \end{aligned} \right\} \quad (36)$$

- it can be observed that this control strategy does not modify the STPHS initial amplitudes and that all the  $v_q^{(s)}$  modified STPHSs remain balanced according to the quantities which multiply  $\phi_q$  are integers. It appears also that the suppression of an harmonic is totally

independent of the constant values so that the experiments are done for  $C_{(x)} = C_{(y)} = 0$ . On the other hand, Eqs 33 and 35 show that the method requires the use of three carriers.

#### 4.1.2. Experimental measurements

**Figure 7a** presents the experimental spectrum for (SΔ) PWM with single carrier and  $r = 1$ . **Figure 7b** and **7c** show the spectra for controls corresponding to the suppression of the harmonics of rank  $x = m + 2$  and  $y = m - 2$  with, respectively,  $\xi_{q(x)} = \phi_q/m$  and  $\xi_{q(y)} = -\phi_q/m$ . These spectra clearly show these deletions although the control laws result from mathematical developments which concern (SS) PWM.

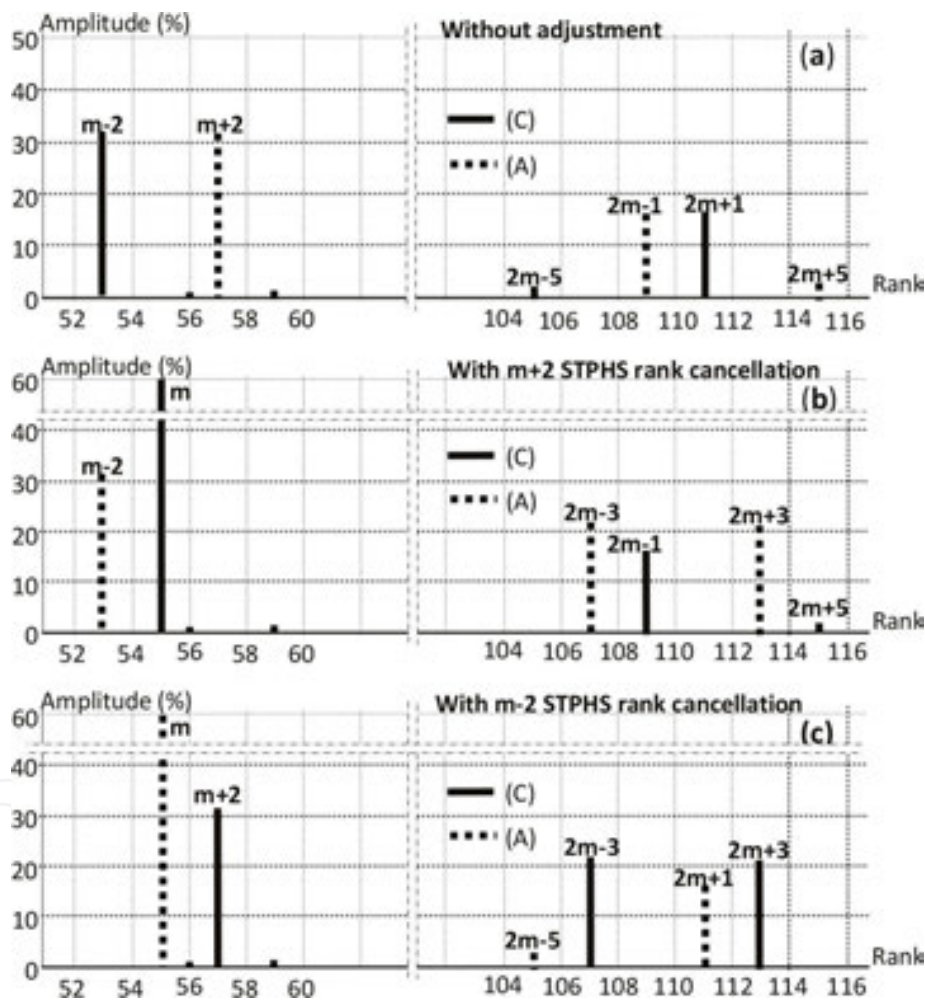


**Figure 7.** Relative experimental  $v_q^{(\Delta)}$  spectra resulting from (b)  $m + 2$  and (c)  $m - 2$  rank harmonic cancellation for  $r = 1$ .

The suppression of  $m + 2$  harmonic rank is accompanied by the disappearance of  $2m + 1$  harmonic rank and the generation of  $m$  and  $2m \pm 3$  harmonic ranks. Similarly, the suppression of  $m - 2$  harmonic rank removes  $2m - 1$  harmonic rank and generates harmonics of rank  $m$  and  $2m \pm 3$ . These particularities as well as the changes on the phase sequences which appear

also on these figures, can easily be justified analytically using Eqs. 34 and 36. Let us note, in accordance with what has already been stated, that the theoretical relative amplitude of  $m$  rank component for (SS) PWM is 100% while, experimentally, for a (SΔ) PWM, it is only 60%.

### 4.2. Suppression of $k_1$ group harmonics

#### 4.2.1. Principle of the $x = 2m + 1$ or $y = 2m - 1$ rank harmonic elimination

- The case of the  $x = 2m + 1$  rank harmonic.  $w_q^{(s)k_1}$  is defined by Eq. (28) with  $n_1 = 1$  and  $n_2 = 0$ . That leads to  $w_q^{(s)k_1} = \hat{w}^{(s)k_1} \sin[(2m + 1)\theta - \phi_q - 2m\xi_q]$ . To make this system (H), the following condition must be satisfied:

$$2m\xi_{q(x)} = -\phi_q + C_{(x)} \tag{37}$$

Thus the modified systems deduced from Eq. (28) can be expressed as:

$$\left. \begin{aligned} w_{q(x)}^{(s)k_1} &= \hat{w}^{(s)k_1} \sin\left[|k_1|\theta + (1 - n_1 + 3n_2)\phi_q / 2 - N^+C_{(x)} / 2 - (1 + n_1)\pi\right] \\ w_{q(x)}^{(s)k_2} &= \hat{w}^{(s)k_2} \sin\left[|k_2|\theta - (2 + n_1 + 3n_2)\phi_q / 2 - N^-C_{(x)} / 2 - n_1\pi\right] \text{ for } k_2 > 0 \\ w_{q(x)}^{(s)k_2} &= \hat{w}^{(s)k_2} \sin\left[|k_2|\theta + (2 + n_1 + 3n_2)\phi_q / 2 + N^-C_{(x)} / 2 - (1 + n_1)\pi\right] \text{ for } k_2 < 0 \end{aligned} \right\} \tag{38}$$

- The case of the  $y = 2m - 1$  rank harmonic.  $w_q^{(s)k_1}$  is defined by Eq. (28) with  $n_1 = 0$  and  $n_2 = 1$  so that  $w_q^{(s)k_1} = \hat{w}^{(s)k_1} \sin[(2m - 1)\theta + \phi_q - 2m\xi_q - \pi]$ . To make this system (H), the following equality must be satisfied:

$$2m\xi_{q(y)} = \phi_q - C_{(y)} \tag{39}$$

The modified systems, deduced from Eq. (28) can be written as:

$$\left. \begin{aligned} w_{q(y)}^{(s)k_1} &= \hat{w}^{(s)k_1} \sin\left[|k_1|\theta - (1 + 3n_1 - n_2)\phi_q / 2 + N^+C_{(y)} / 2 - (1 + n_1)\pi\right] \\ w_{q(y)}^{(s)k_2} &= \hat{w}^{(s)k_2} \sin\left[|k_2|\theta - (2 + 3n_1 + n_2)\phi_q / 2 + N^-C_{(y)} / 2 - n_1\pi\right] \text{ for } k_2 > 0 \\ w_{q(y)}^{(s)k_2} &= \hat{w}^{(s)k_2} \sin\left[|k_2|\theta + (2 + 3n_1 + n_2)\phi_q / 2 - N^-C_{(y)} / 2 - (1 + n_1)\pi\right] \text{ for } k_2 < 0 \end{aligned} \right\} \tag{40}$$

- As previously:
  - the constants do not affect the results, so they will be assumed to be null
  - Equations 37 and 39 show that the method requires the use of three carriers

It can also be observed that this control strategy does not modify the STPHS initial amplitudes but that the quantities which multiply  $\phi_q$  are not integers unless if the quantities between brackets are even. That means that many systems initially balanced become unbalanced. **Tables 5** and **6** show the modifications of  $w_q^{(s)k}$  STPHS phase sequences, respectively, for  $2m + 1$  and  $2m - 1$  harmonic rank cancellations. HCA means that a system initially (C), (A), or (H) becomes unbalanced. Only the harmonic components which do not depend on  $m$  ( $k_2$  group) and those around  $6m$  ( $k_1$  group), keep the same characteristics.

		(a) $k_1$ group				(b) $k_2$ group			
$n_1$		0	1	2	3	0	1	2	3
$n_2$	0	m (H)→(HCA)	2m + 1 (C)→(H)	3m + 2 (A)→(HCA)	4m + 3 (H)→(D)	1 (C)	m + 2 (A)→(HCA)	2m + 3 (H)→(A)	3m + 4 (C)→(HCA)
	1	2m - 1 (A)→(C)	3m (H)→(HCA)	4m + 1 (C)→(A)	5m + 2 (A)→(HCA)	-m + 2 (C)→(HCA)	3 (H)	m + 4 (C)→(HCA)	2m + 5 (A)→(C)
	2	3m - 2 (C)→(HCA)	4m - 1 (A)→(H)	5m (H)→(HCA)	6m + 1 (C)	-2m + 3 (H)→(A)	-m + 4 (A)→(HCA)	5 (A)	m + 6 (H)→(HCA)
	3	4m - 3 (H)→(C)	5m - 2 (C)→(HCA)	6m - 1 (A)	7m (H)→(HCA)	-3m + 4 (A)→(HCA)	-2m + 5 (C)→(H)	-m + 6 (H)→(HCA)	7 (C)

**Table 5.** Theoretical impact of the  $2m + 1$  harmonic (group  $k_1$ ) suppression on the  $w_q^{(s)}$  spectral content.

		(a) $k_1$ group				(b) $k_2$ group			
$n_1$		0	1	2	3	0	1	2	3
$n_2$	0	m (H)→(HCA)	2m + 1 (C)→(A)	3m + 2 (A)→(HCA)	4m + 3 (H)→(A)	1 (C)	m + 2 (A)→(HCA)	2m + 3 (H)→(C)	3m + 4 (C)→(HCA)
	1	2m - 1 (A)→(H)	3m (H)→(HCA)	4m + 1 (C)→(H)	5m + 2 (A)→(HCA)	-m + 2 (C)→(HCA)	3 (H)	m + 4 (C)→(HCA)	2m + 5 (A)→(H)
	2	3m - 2 (C)→(HCA)	4m - 1 (A)→(C)	5m (H)→(HCA)	6m + 1 (C)	-2m + 3 (H)→(C)	-m + 4 (A)→(HCA)	5 (A)	m + 6 (H)→(HCA)
	3	4m - 3 (H)→(A)	5m - 2 (C)→(HCA)	6m - 1 (A)	7m (H)→(HCA)	-3m + 4 (A)→(HCA)	-2m + 5 (C)→(A)	-m + 6 (H)→(HCA)	7 (C)

**Table 6.** Theoretical impact of the  $2m - 1$  harmonic (group  $k_1$ ) suppression on the  $w_q^{(s)}$  spectral content.

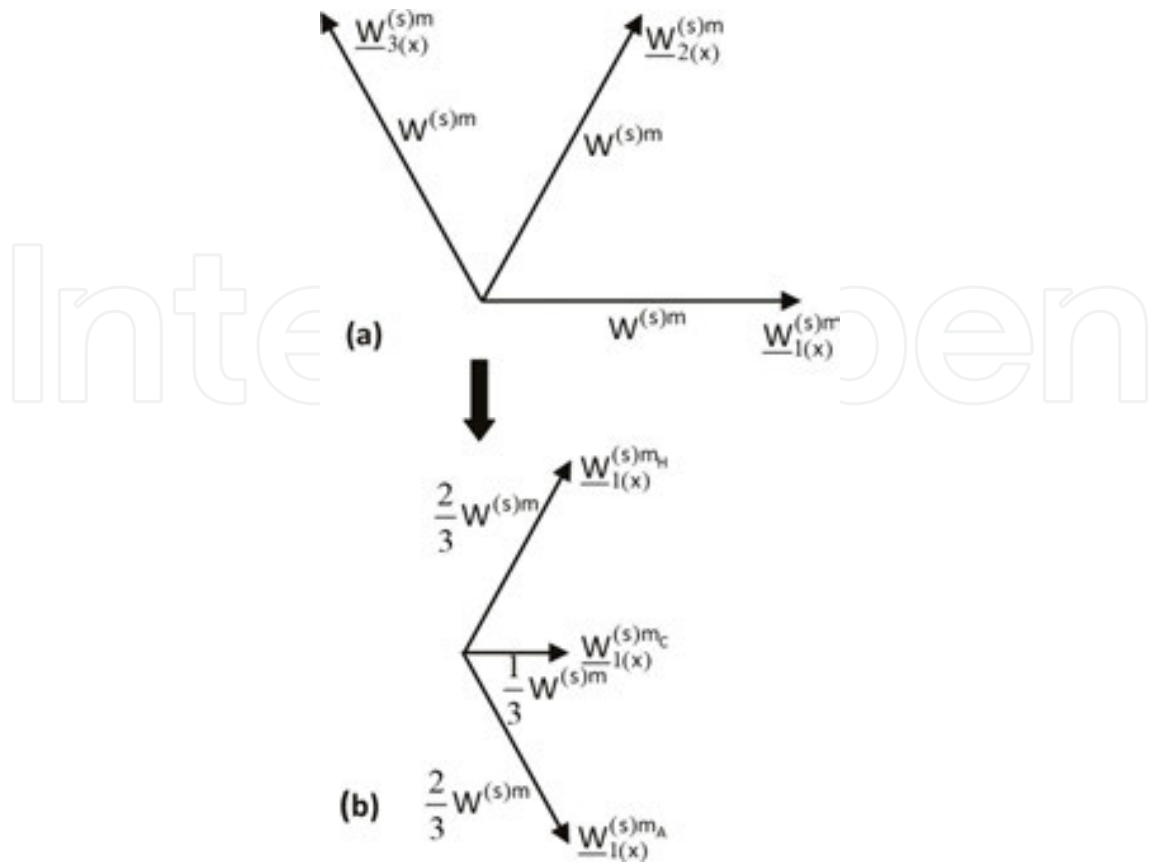


Figure 8. Cancellation of the harmonic  $x = 2m + 1$ : Components (C), (A) and (H) of  $m$  rank STPHS.

From magnetic noise point of view, it is necessary to characterize each STPHS with its (C), (A) and (H) components. They result from the following classical expressions which use time phasor variables and where  $a = \exp(j2\pi/3)$ :

$$\left. \begin{aligned} \underline{W}_{1(xor\gamma)}^{(s)k_C} &= (\underline{W}_{1(xor\gamma)}^{(s)k} + a\underline{W}_{2(xor\gamma)}^{(s)k} + a^2\underline{W}_{3(xor\gamma)}^{(s)k}) / 3 \\ \underline{W}_{1(xor\gamma)}^{(s)k_A} &= (\underline{W}_{1(xor\gamma)}^{(s)k} + a^2\underline{W}_{2(xor\gamma)}^{(s)k} + a\underline{W}_{3(xor\gamma)}^{(s)k}) / 3 \\ \underline{W}_{1(xor\gamma)}^{(s)k_H} &= (\underline{W}_{1(xor\gamma)}^{(s)k} + \underline{W}_{2(xor\gamma)}^{(s)k} + \underline{W}_{3(xor\gamma)}^{(s)k}) / 3 \end{aligned} \right\} \quad (41)$$

Let us consider, for example, the  $x = 2m + 1$  harmonic rank suppression and the modified system given by Eq. (38). The “ $m$ ” harmonic rank belongs to the  $k_1$  group, and it is defined for  $n_1 = n_2 = 0$  (Table 5). Considering Eq. (37) for  $C_{(x)} = 0$ , this “ $m$ ” harmonic rank system can be expressed as:

$$w_{q(x)}^{(s)m} = \hat{w}^{(s)m} \sin\left(m\theta + (q-1)\frac{\pi}{3} - \pi\right) \quad (42)$$

It leads to **Figure 8(a)**, where the modulus of each time phasor variable is defined using its RMS value:  $W^{(s)m} = \hat{w}^{(s)m}/\sqrt{2}$ . Eq. (41) leads to the Phase 1 time phasor variable of each component given in **Figure 8(b)**. One can note that (H) and (A) systems have the same  $2W^{(s)m}/3$  modulus, the (C) modulus is  $W^{(s)m}/3$ . As, theoretically, the relative amplitude of the  $m$  harmonic is equal to 1 (**Table 4**), one can deduced that the relative absolute values of the (C) and (A) systems of  $v^{(s)m}$  are, respectively, equal to 33.3 and 66.6%.

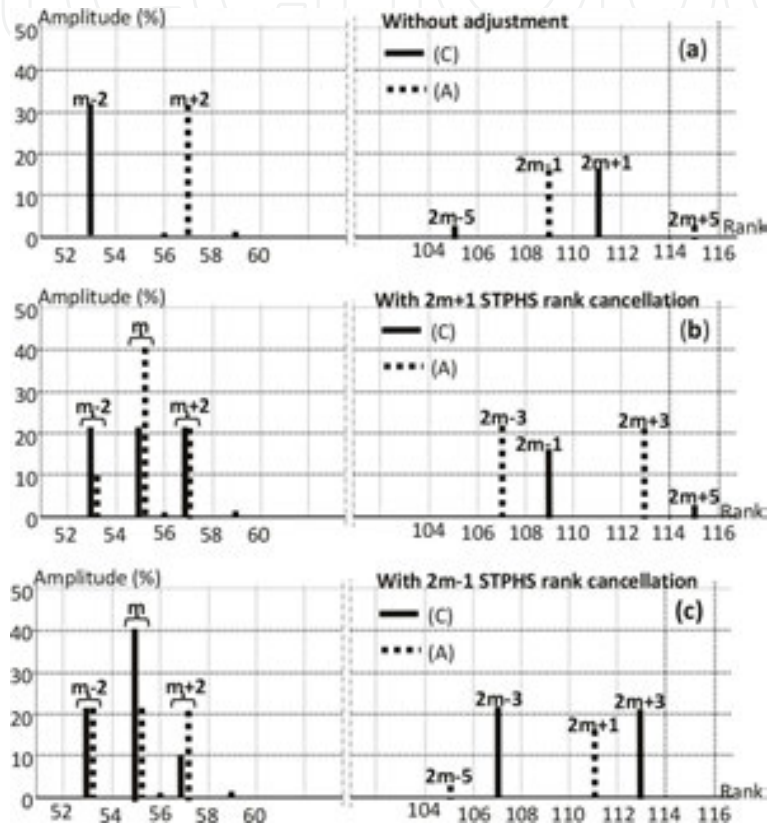


**Figure 9.** Relative experimental  $v_q^{(\Delta)}$  spectra for  $m = 55$  and  $r = 1$  resulting from: (b)  $2m + 1$  and (c)  $2m - 1$  rank harmonic cancellation.

#### 4.2.2. Experimental measurements

- First, verifications about  $v_q^{(\Delta)}$  make it possible to show, for the unbalanced harmonic systems, that, for a harmonic, the spectral components have the same amplitudes on the three phases. As the expressions deduced from the (SS) PWM lead to accurate values of the phase angles, the authors have used expression 41 to characterize the (C) and (A) amplitudes of the  $v_q^{(\Delta)}$  systems. **Figures 9b** and **c** show the experimental  $v_q^{(\Delta)}$  spectrum thus obtained for, respectively,  $2m + 1$  and  $2m - 1$  harmonic rank cancellation. This suppression leads:

- to new components of rank  $2m \pm 3$  which are (C) or (A), as determined with the analytical model,
- to a unbalanced “m” rank component which is constitutes of (C) and (A) three-phase systems. The amplitudes of these latter present a sum always equal to 100%.

The validity of the proposed method is established as well as the theoretical approach proposed for characterizing the STPHS phase sequences. It is now possible to consider more complex control strategies in order, for example, to mitigate some of the negative effects caused by the removal of a single harmonic as the generation of new harmonic ranks in  $v_q$  spectral content. To do that, a procedure has been developed: the carrier phase jump which is presented in the following section.

## 5. Carrier-phase jump

To present this method, it will be shown how it is possible to minimize, for example, the effects of the reappearance of the harmonic system of rank “m” when the harmonic system of rank  $m + 2$  is suppressed. The principle consists in associating with this harmonic of  $m + 2$  rank, harmonic of  $m - 2$  rank, and alternately removing these harmonic systems. By exploiting the degree of freedom introduced by the constants makes it possible to optimize the minimization of harmonic of “m” rank.

### 5.1. Principle

The rank  $x = m + 2$  harmonic is suppressed during the first  $v_q^{ref}$  period and the rank  $y = m - 2$  harmonic during the second one. This transition is accompanied by transitions on all the modified STPHSs. Taking into account Eqs 34 and 36 leads to expressing a modified  $k$  rank STPHS using the general form:

$$w_{q(xory)}^{(s)k} = \hat{w}^{(s)k} \sin \left[ k\theta - \psi_{q(xory)}^{(s)k} \right] \quad (43)$$

$\psi_{q(xory)}^{(s)k}$ , defined by identification, depends on  $\phi_q$ ,  $C_{(x)}$  and  $C_{(y)}$ . The Fourier series of resulting  $w_{q(x,y)}^{(s)k}$  signal requires considering an interval that corresponds to  $2T$ . The two expressions of this signal on the considered  $2T$  interval are the following:

$$\left. \begin{aligned} w_{q(x)}^{(s)k} &= \hat{w}^{(s)k} \sin \left[ 2k(\theta - \psi_{q(x)}^{(s)k} / 2k) \right] \\ w_{q(y)}^{(s)k} &= \hat{w}^{(s)k} \sin \left[ 2k(\theta - \psi_{q(y)}^{(s)k} / 2k) \right] \end{aligned} \right\} \quad (44)$$

Let us denote  $h^k$  as  $w_{q(x,y)}^{(s)k}$  rank harmonic. If  $t = 0$  is the instant which corresponds to the passage of  $w_{q(x)}^{(s)k}$  to  $w_{q(y)}^{(s)k}$ , it can be written as:

$$w_{q(x,y)}^{(s)k} = \sum_{h^k=1}^{\infty} \hat{w}_{q(x,y)}^{(s)k,h^k} \cos(h^k \theta - \beta_{q(x,y)}^{(s)k,h^k}) \quad (45)$$

where

$$\left. \begin{aligned} \hat{w}_{q(x,y)}^{(s)k,h^k} &= \hat{w}^{s(k)} \sqrt{(A_q^{k,h^k})^2 + (B_q^{k,h^k})^2} \\ \text{tg} \beta_{q(x,y)}^{(s)k,h^k} &= B_q^{k,h^k} / A_q^{k,h^k} \end{aligned} \right\} \quad (46)$$

**Table 7** gives the expressions of  $A_q^{k,h^k}$  and  $B_q^{k,h^k}$  with  $\psi_{q+}^{(s)k} = (\psi_{q(x)}^{(s)k} + \psi_{q(y)}^{(s)k})/2$ ,  $\psi_{q-}^{(s)k} = (\psi_{q(x)}^{(s)k} - \psi_{q(y)}^{(s)k})/2$

	$A_q^{k,h^k}$	$B_q^{k,h^k}$	$\hat{w}_{q(x,y)}^{(s)k,h^k}$	$\beta_{q(x,y)}^{(s)k,h^k}$
$h^k \text{ even} \neq 2k$	0	0	0	
$h^k \text{ odd}$	$8k \frac{\sin \psi_{q+}^{(s)k} \sin \psi_{q-}^{(s)k}}{(2k+h^k)(2k-h^k)\pi}$	$-4h^k \frac{\cos \psi_{q+}^{(s)k} \sin \psi_{q-}^{(s)k}}{(2k+h^k)(2k-h^k)\pi}$	$\hat{w}^{(s)k} \frac{2}{\eta\pi}  \sin \psi_{q-}^{(s)k} $	$\psi_{q+}^{(s)k} + \pi/2$
$h^k = 2k$	$-\sin \psi_{q+}^{(s)k} \cos \psi_{q-}^{(s)k}$	$\cos \psi_{q+}^{(s)k} \cos \psi_{q-}^{(s)k}$	$\hat{w}^{(s)k}  \cos \psi_{q-}^{(s)k} $	$\psi_{q+}^{(s)k} + \pi/2$

**Table 7.** x→y jump—Expressions of the Series Fourier coefficients for a  $k$  rank term.

On  $T$ , for given  $k$ , this method leads to associate with the initial harmonic components defined by Eq. (44):

- a component of Integer (I) rank “k” defined by the values given in **Table 7** for  $h^k = 2k$ ,
- components defined for  $h^k$  odd, leading to harmonics of Non-Integer (NI) ranks.

The characteristics of these components are defined by the values given in the first row for  $h^k$  odd in **Table 7**.

As  $h^k$  odd can be expressed by  $h^k = 2k \pm \eta$  with  $\eta$  odd, these NI rank harmonics are defined on "T" by  $k \pm \eta/2$ .

Insofar as these harmonics present significant values only for  $\eta$  first values, the second row for  $h^k$  odd gives the simplified expressions valid only under these conditions.

So the (I) rank "k" component is surrounded by NI rank harmonics.

Let us point out that for the fundamental component ( $k = 1$ ), the expressions of  $w_{q(x)}^{(s)1}$  and  $w_{q(y)}^{(s)1}$  that can be deduced from Eqs 34 and 36 are the same. Thus, the carrier-phase jump has no effect on this component.

## 5.2. Numerical applications

The expressions of  $\psi_{q(x)}^{(s)k}$  and  $\psi_{q(y)}^{(s)k}$ , grouped in **Table 8**, are obtained:

- by identification considering Eqs. (34) and (36), with  $k$  taking successively the values  $m \pm 2$ ,  $m$ ,  $2m \pm 1$  and  $2m \pm 3$ ,
- and by characterizing the quantities  $\varepsilon_{q(xory)}$  with their general expressions given by Eqs. (33) and (35).

The  $\psi_{q+}^{(s)k}$  and  $\psi_{q-}^{(s)k}$  expressions, defined in functions of  $C^+ = C_{(x)} + C_{(y)}$  and  $C^- = C_{(x)} - C_{(y)}$  are also given in **Table 8**. These mathematical developments have a notable interest because the  $h^k$  rank harmonic amplitudes, which differ with the value of  $q$ , only depend on  $\psi_{q-}^{(s)k}$  (see **Table 7**) and thus on  $C^+$ . The phases depends only on  $\psi_{q+}^{(s)k}$  and thus on  $C^-$ .

**Figure 10** shows the variations of  $|\cos\psi_{q-}^{(s)k}|$  and  $|\sin\psi_{q-}^{(s)k}|$  with  $C^+$  for the previous "k" values and the three "q" values. In order to exploit these curves, it should be noted that for  $k = 2m \pm 1$  and  $2m \pm 3$ , the horizontal scale must be divided by 2. The harmonic amplitudes are obtained by multiplying these quantities by the coefficients given in **Table 7**. As shown in **Figure 10**, for a given "q" value, the maximal value of the (I) rank "k" harmonic is associated with (NI) harmonics whose values are null.

The new STPHSs are all unbalanced, therefore, they can be defined by their (C), (A), and (H) components. The analysis made on these component moduli, and more especially on  $|\cos\psi_{q-}^{(s)k}|$  and  $|\sin\psi_{q-}^{(s)k}|$ , for a given value of the (I) rank "k" component, shows that the coefficients which intervene in their definitions (multiplying the modulus given in **Table 7**) are independent from  $h^k$ , as well as the values given to  $C^+$  and  $C^-$ . The numerical values of these coefficients are given also in **Table 8**.

	$\psi_{q(x)}^{(s)k}$	$\psi_{q(y)}^{(s)k}$	$\psi_{q+}^{(s)k}$	$\psi_{q-}^{(s)k}$	(C)	(A)	(H)
$m - 2$	$-\phi_q - C_{(x)} + \pi$	$C_{(y)} + \pi$	$\pi - (\phi_q + C^-)/2$	$-(\phi_q + C^+)/2$	0	0.5	0.5
$m + 2$	$-C_{(x)} + \pi$	$\phi_q + C_{(y)} + \pi$	$\pi + (\phi_q - C^-)/2$	$-(\phi_q + C^+)/2$	0.5	0	0.5
$m$	$\phi_q - C_{(x)} + \pi$	$-\phi_q + C_{(y)} + \pi$	$\pi - C^-$	$\phi_q - C^+/2$	0.5	0.5	0
$2m - 1$	$\phi_q - 2C_{(x)} + \pi$	$2C_{(y)} + \pi$	$\pi - C^- + \phi_q/2$	$-C^+ + \phi_q/2$	0.5	0	0.5
$2m + 1$	$-2C_{(x)}$	$-\phi_q + 2C_{(y)}$	$\pi - C^- + \phi_q/2$	$-C^+ + \phi_q/2$	0	0.5	0.5
$2m - 3$	$-\phi_q - 2C_{(x)} + \pi$	$\phi_q + 2C_{(y)} + \pi$	$\pi - C^-$	$-\phi_q - C^+$	0.5	0.5	0
$2m + 3$	$-\phi_q - 2C_{(x)}$	$\phi_q + 2C_{(y)}$	$-C^-$	$-\phi_q - C^+$	0.5	0.5	0

**Table 8.** Expressions of  $\psi_{q(x)}^{(s)k}$  and  $\psi_{q(y)}^{(s)k}$  and (C), (A) and (H) component characterization.

First, one can note that a carrier-phase jump which involves in the transition an (H) STPHS, leads to corresponding  $w_q^{(s)}$  STPHS which contains also (H) component. In this case, the  $v_q^{(s)}$  STPHSs are balanced as shown in **Table 8**. For all the other cases, the  $v_q^{(s)}$  STPHSs are unbalanced.

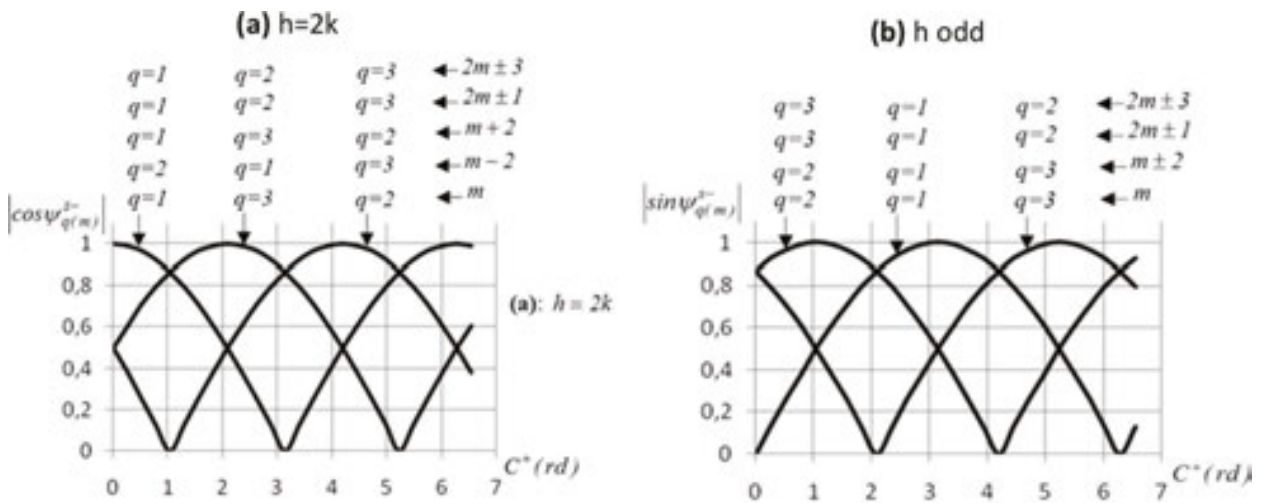


**Figure 10.** Variations of  $|\cos\psi_{q(m)}^{S-}|$  and  $|\sin\psi_{q(m)}^{S-}|$  with  $C^+$ .

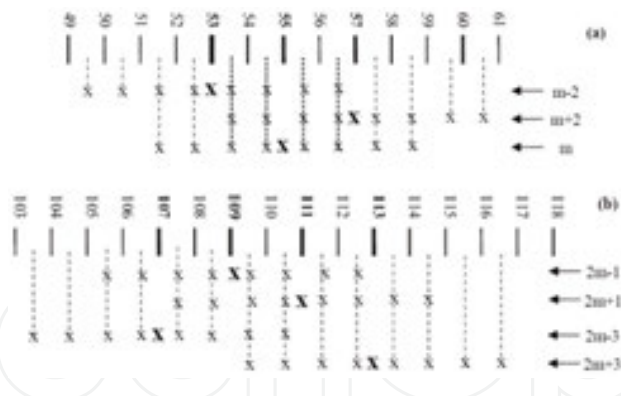


Figure 11. NI rank harmonics: (a) around  $m$ ; (b) around  $2m$ .

The NI rank harmonics are subject to the second remark. They form balanced STPHSs for the  $m \pm 2$  and  $2m \pm 1$  (I) rank harmonics, and unbalanced STPHSs for all the other considered (I) rank harmonics. These harmonics combine together as it appears in **Figure 11** which considers the quantities that appear around  $m$  (**Figure 11a**) and around  $2m$  (**Figure 11b**). For this study, the number of NI rank harmonics considered is limited to the  $\eta$  first four values. It results that the characteristic predetermination of NI rank harmonics needs to add several terms taking into account the  $\beta_{q(x,y)}^{(s)k}, h^k$  quantities given in **Table 7**, which depend on  $\psi_{q+}^{(s)k}$ , and consequently on  $C^-$  quantities as it appears in **Table 8**.

### 5.3. Experimental validation for (SS) PWM

The aim of these applications is to validate the theoretical developments corresponding to the previous case ( $m = 55, r = 1, x = m + 2$  and  $y = m - 2$ ).

- First, the constants are such as  $C_{(x)} = C_{(y)} = 0$ , defining  $C^+ = 0$ . The analytical developments lead to the  $v_{q(x,y)}^{(s)}$  component relative amplitudes in % given in **Table 9**. The quantities for NI rank harmonics are calculated for  $\eta = 1$ . Let us point out that only two lines,  $q = 1$  and  $q = 2$ , constitute **Table 9** because, for this case, the  $q = 2$  and 3 components present identical amplitudes. When the numerical values for  $q = 1$  and 2 are the same, the STPHSs are balanced.

	$m(100\%)$		$m \pm 2(33.3\%)$		$2m \pm 1(33.3\%)$		$2m \pm 3(20\%)$	
	I	NI	I	NI	I	NI	I	NI
$q = 1$	100	0	16.65	10.64	16.65	10.64	20	0
$q = 2$	50	55	16.65	10.64	16.65	10.64	10	11.1

Table 9.  $v_{q(x,y)}^{(s)}$  component relative amplitudes for  $C^+ = 0$ .

The  $v_{q(x,y)}^{(s)}$  spectra corresponding to this (SS) PWM are given in **Figure 12**. Let us consider the (I) rank harmonics. One can note a very good correspondence between the predetermined values and those deduced from the spectra.

Concerning the NI rank harmonics, let us consider the  $m + 0.5$  rank harmonic which results from the combination of three terms as it appears in **Figure 11a**:

- the harmonic related to  $k = m$  for  $\eta = 1$ , whose relative amplitude is 0% for  $q = 1$  and 55% for  $q = 2$  and 3,
- the harmonic related to  $k = m + 2$  for  $\eta = 2$ , whose relative amplitude is 5.32% for the three phases,
- the harmonic related to  $k = m - 2$  for  $\eta = 3$ , whose relative amplitude is 3.55% for the three phases.

The approach is identical to characterize  $m - 0.5$  rank harmonic. One can estimate that the components of  $m \pm 0.5$  ranks have an amplitude of a few percents for  $q = 1$  and an amplitude of the order of 50–60% for  $q = 2$  and 3. These quantities correspond to those measured on the spectra. A similar approach for the other NI harmonics leads to similar conclusions.

- The constants are adjusted such as  $C_{(x)} = 0$  et  $C_{(y)} = \pi$ , leading to  $C^+ = \pi$ . **Table 10** presents the  $v_{q(x,y)}^{(s)}$  component relative amplitudes given in % deduced from the analytical developments. Only the harmonics around "m" rank are considered because taking into account the periodicity of curves presented in **Figure 10**, the spectral content around  $2m$  is the same than the content obtained for  $C^+ = 0$ . The spectral contents presented in **Figure 13**, which concern only harmonics around "m", show the good correspondence between predetermined and measured values that validates the analytical relationships.

	$m(100\%)$		$m \pm 2(33.3\%)$	
	I	NI	I	NI
$q = 1$	0	64	16.65	10.64
$q = 2$	86.6	32	16.65	10.64

**Table 10.**  $v_{q(x,y)}^{(s)}$  component relative amplitudes for  $C^+ = \pi$ .

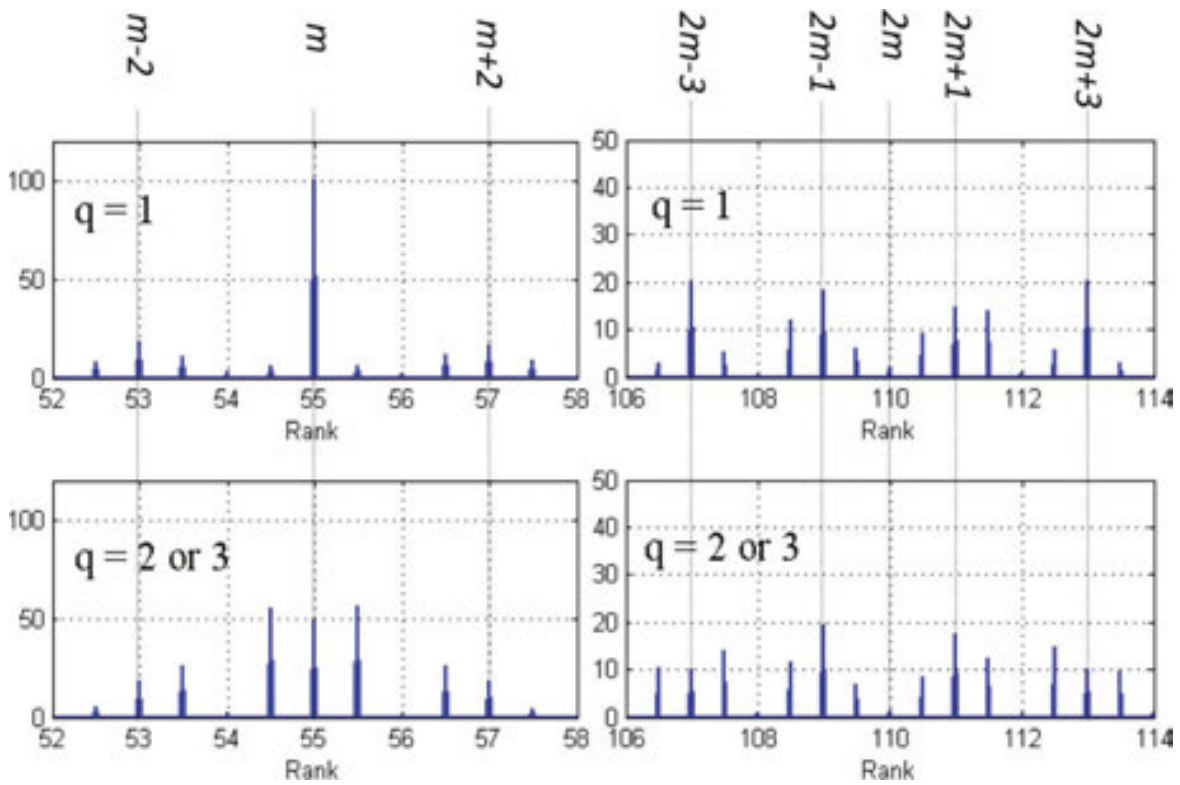


Figure 12. (SS) PWM,  $v_{1and2}^{(s)}$  spectra around  $m$  and  $2m$  for  $C^+ = 0$ .

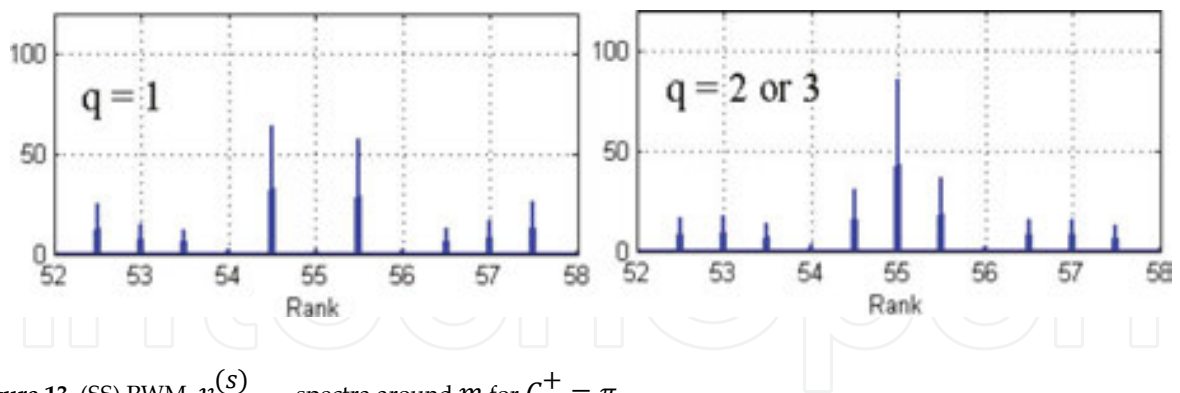


Figure 13. (SS) PWM,  $v_{1and2}^{(s)}$  spectra around  $m$  for  $C^+ = \pi$ .

#### 5.4. Experimental validation for (SΔ) PWM

The spectra measured for a (SΔ) PWM, given in **Figures 14** and **15**, have the same properties when the constants are changed; only the amplitudes are modified. For example, the spectra shown in **Figures 14** and **15** correspond to the spectra given in **Figures 12** and **13** obtained for a (SS) PWM.

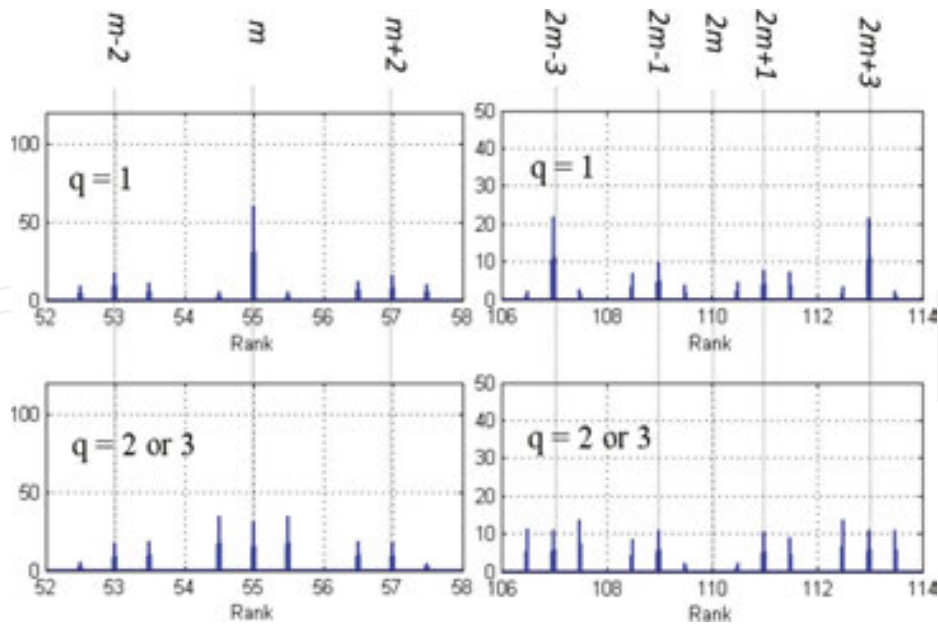


Figure 14. (SΔ) PWM,  $v_{1and2}^{(\Delta)}$  spectra around  $m$  and  $2m$  for  $C^+ = 0$ .

The validity of developments made on a (SS) PWM to characterize the spectral content of a (SΔ) PWM is again demonstrated on this quite particular control technique which results, compared with the original spectrum shown in Figure 6a, to a spread spectrum with a significant changes of the amplitudes of some initial harmonic components.

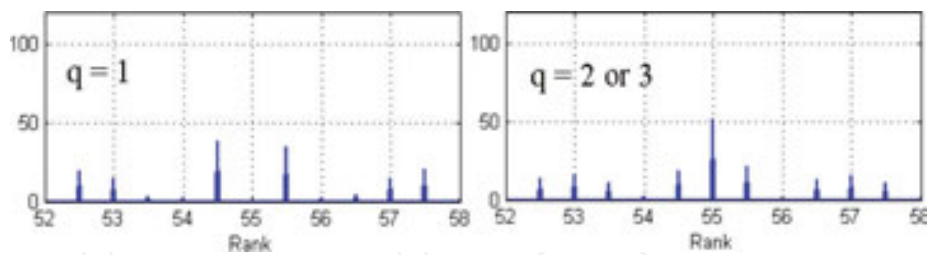


Figure 15. (SΔ) PWM,  $v_{1and2}^{(\Delta)}$  spectra around  $m$  for  $C^+ = \pi$ .

## 6. Use of carriers of different frequencies

### 6.1. Principle

The principle is shown considering the theoretical model of a (SS) PWM. The modulation index  $m_q$  concerns the phase “q”. It will be supposed that  $m_q$  differs with “q” satisfying, for example, the equalities  $m_{q-1} = m - \Delta m$ ,  $m_{q+1} = m + \Delta m$ . Table 4 which gives the  $w_q^{(s)}$  harmonic content shows that

- the harmonic of ranks 1, 3, 5, 7, ..., are independent of the values given to  $m_q$  and, thus, the fundamental is not modified when carrier frequencies are different
- the other harmonics define groups of components centered:

$$\left. \begin{aligned}
 &\text{-on } m_q : m_q, m_q \pm 2, m_q \pm 4, m_q \pm 6, \\
 &\text{-on } 3m_q : 3m_q, 3m_q \pm 2, 3m_q \pm 4, 3m_q \pm 6, \\
 &\text{-on } 5m_q : 5m_q, 5m_q \pm 2, 5m_q \pm 4, 5m_q \pm 6, \\
 &\text{-on } 2m_q : 2m_q \pm 1, 2m_q \pm 3, 2m_q \pm 5, \\
 &\text{-on } 4m_q : 4m_q \pm 1, 4m_q \pm 3, 4m_q \pm 5, \\
 &\text{-on } 6m_q : 6m_q \pm 1, 6m_q \pm 3, 2m_q \pm 5,
 \end{aligned} \right\} \quad (47)$$

The initial structure in **Figure 3a** can also be presented using the scheme given in **Figure 16** where a harmonic, function of  $m_q$  must also be distinguished according to the considered phase "q". It results that an harmonic rank will be denoted using two superscripts  $k^q, j$ .

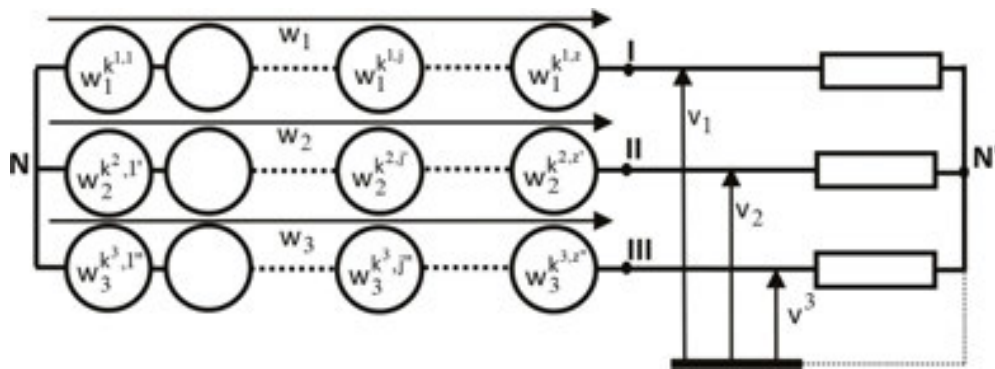


**Figure 16.** Equivalent structure of the converter associated to the IM.

To analyze how an harmonic of rank "k" modifies the behavior of the load, the superposition principle is applied and the generator giving a signal of frequency kf is searched for each phase. Then, after identification of these different generators, all the others are switched off. Let us underline that this approach concerns all the harmonics different from the components of rank 1, 3, 5, 7 ..., for the latter, the voltage STPHSs applied to the load will be balanced because the (H) component cannot exist at the terminal connections of the load.

It results that an harmonic of "k" rank can, for example, concerning the Phase 1, belong to the group of components centered on  $m_1$  and, concerning the Phase 2, to the group of component centered on  $2m_2$ . This example shows that three cases have to be considered:

- *Case 1.* If a STPHS of rank "k," which exists on a phase, is also on the two other phases, then the structure in **Figure 17a** is obtained where the three generators constitute an imbalanced three-phase system where  $k^1, j = k^2, j' = k^3, j'' = k$ .

- Case 2. If a STPHS of rank “k,” which exists on Phase 1, is only on one of the two other phases (Phase 2, for example), then the structure in **Figure 17b** is obtained where  $k^{1,j} = k^{2,j'} = k$  and where the RMS voltage generators have, a priori, no link.
- Case 3. If a STPHS of rank “k,” which exists on Phase 1, is not on the two other phases, then the structure in **Figure 17c** has to be considered where  $k^{1,j} = k$ .
- The Case 1 has already been considered: the intermediate system has to be decomposed in (C), (A), and (H) components using Eq. (41) and considering that only the (C) and (A) systems are applied to the load.
- For the Case 2 it appears, considering the example given in **Figure 17b**, that  $\underline{V}_1^k = (2\underline{W}_1^k - \underline{W}_2^k)/3$ ,  $\underline{V}_2^k = (2\underline{W}_2^k - \underline{W}_1^k)/3$ ,  $\underline{V}_3^k = -(\underline{W}_1^k + \underline{W}_2^k)/3$ . This STPHS that appears at the load inputs is unbalanced without (H) component.
- Concerning the Case 3, **Figure 17c** leads to  $\underline{V}_1^k = 2\underline{W}_1^k/3$ ,  $\underline{V}_2^k = -\underline{W}_1^k/3$ . As previously, this STPHS that appears at the load inputs is unbalanced without (H) component.
- When the structures of circuits in **Figures 17b** and **17c** are changed (by considering, for example, that the generator of **Figure 17c** that supplies the circuit is not connected to Phase 1 but to Phase 2, the previous equations can still be used but need an adaptation of the indexes.

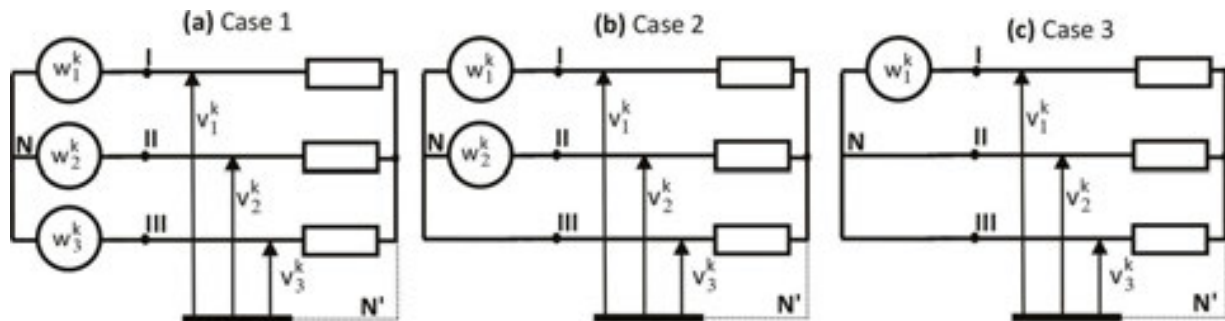


Figure 17. Different configurations of the equivalent circuit with  $k$ .

## 6.2. Numerical application—experimental validation

The case of  $m_1 = 45$ ,  $m_2 = 55$ , and  $m_3 = 65$  for  $f = 50$  Hz and  $r = 1$  is considered.

### 6.2.1. (SS) PWM

Taking into account Eq. (47), it appears immediately that all the harmonics have odd ranks. Considering only the two first groups of components, the theoretical spectra given in **Figure 18** show that:

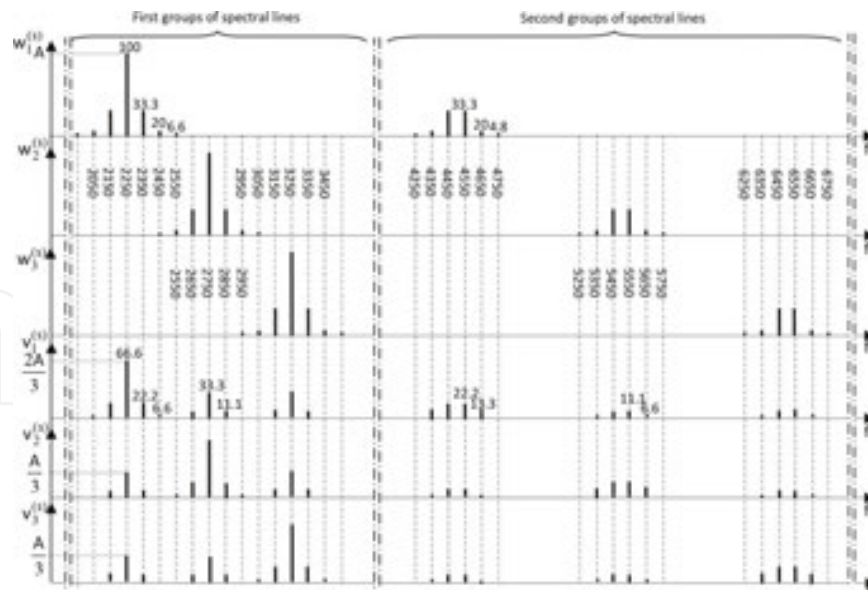


Figure 18. Principle of frequency shift carriers for (SS) PWM,  $f = 50$  Hz and  $m_1 = 45$ ,  $m_2 = 55$  et  $m_3 = 65$ .

- For the first group of components, the equivalent circuits are the same as the circuit given in **Figure 17c**. The component  $m_1 f$  (2250 Hz) of  $w_1^{(s)}$ , whose theoretical amplitude is 100% (**Table 4**), is dispatched on  $v_q^{(s)}$  with an amplitude of 66.6% for  $q = 1$  and 33.3% for  $q = 2$  and 3. Concerning  $w_q^{(s)}$ , there is, for example, coincidences of the component  $(m_1 + 4)f$  of  $w_1^{(s)}$  with the component  $(m_2 - 6)f$  of  $w_2^{(s)}$  (2450 Hz). However, the amplitudes of these theoretical components are, respectively, 6.6 and 2.8% so that the resulting effect to be analyzed with the scheme given in **Figure 17b** will nearly not appear in the  $v_q^{(s)}$  spectra. Consequently, this interaction is ignored.

Coincidences exist, in general, for all the components, but if the quantities  $m_q$  are chosen correctly, they involve two generators on the three that have almost zero voltages so that one has only to consider the configuration given in **Figure 17c**.

- The previous remark can be generalized for all the second groups of components shown in **Figure 18**. It must be noted that the third group of component (not shown) modifies significantly the amplitudes of the components between 6250 and 6750 Hz. Indeed, if the third group is considered for  $q = 1$ , the components which will interfere with the existing components have, for the most important of them, the following characteristics:

- $3m_1 f = 6750$  Hz whose theoretical amplitude is 11.1%,
- $(3m_1 - 2)f = 6650$  Hz whose theoretical amplitude is 20%
- $(3m_1 - 4)f = 6550$  Hz whose theoretical amplitude is 14.3%
- $(3m_1 - 6)f = 6450$  Hz whose theoretical amplitude is 3.7%

In this case, the analysis has to exploit the scheme in **Figure 17b**. It results that what appears in Phase 1 is different from what can be observed on Phases 2 and 3 which are not modified by the third group of components.

### 6.2.2. (SΔ) PWM

The experimental  $v_2^{(\Delta)}$  and  $v_3^{(\Delta)}$  spectra (without decomposition considering (C) and (A) systems) for a (SΔ) PWM for the conditions corresponding to the theoretical study, are shown in **Figure 19**. The spectral distribution in **Figure 18** is verified, except for the amplitudes.

This technic which consists in using three carriers of different frequencies leads, if comparing to a classical (SΔ) PWM, to a splintering of the spectrum with a decrease of the initial components.

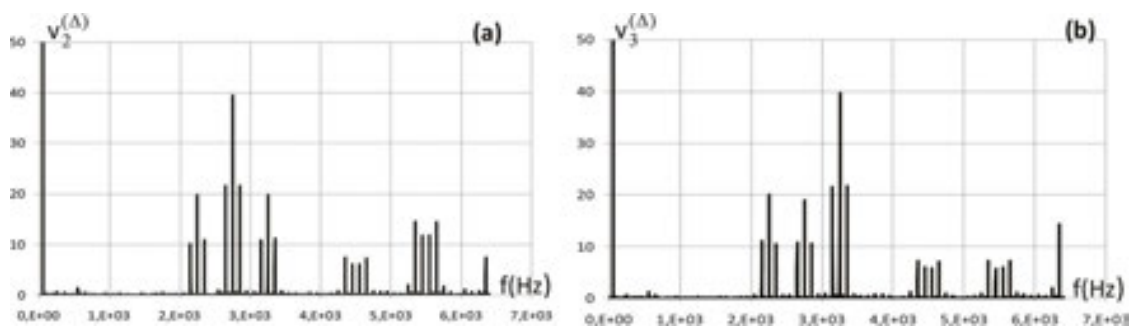


**Figure 19.** Experimental validation of the principle using carriers of different frequencies for  $f = 50$  Hz and  $m_1 = 45$ ,  $m_2 = 55$  and  $m_3 = 65$ .

Concerning this presentation, it seems difficult to develop further as the number of combinations on the choice of values to assign to the mq quantities is infinite justifying that, from an analytical point of view, only the principle is presented.

## 7. Experiments on noise and vibrations

Certain machines have been redesigned in order to be more efficient when they operate at variable speed using PWM inverters. Precautions have also been taken to minimize noise problems. Unfortunately, for some of them, severe acoustic problems due to the STPHSs appear when they operate. It is in this context that the presented methods were developed. For confidential reasons, it is not possible to give the results about these specific experiments. Thus the presented results concern 2 IMs available in our laboratory with the following characteristics:

M1: cage IM—15 kW, 50 Hz,  $p = 2$ , 1456 rpm, 380 V, 24.8A,  $N^s = 48$ ,  $N^r = 36$ .

M2: wound rotor IM—15 kW, 50 Hz,  $p = 3$ , 950 rpm, 365 V, 28A,  $N^s = 72$ ,  $N^r = 54$ .



Figure 20. Positions of the accelerometers on M1.

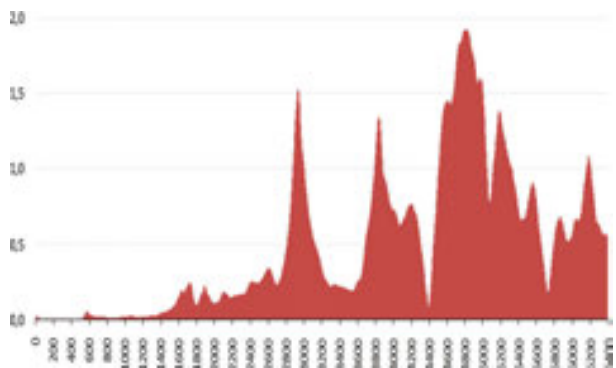


Figure 21. Frequency response of the M1 outer casing.

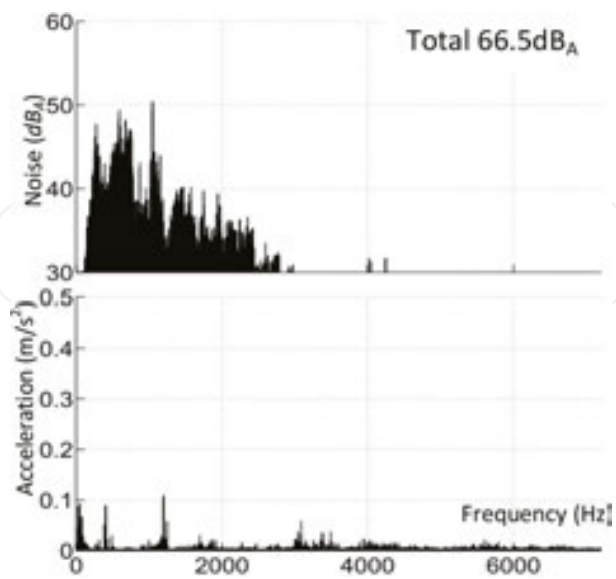


Figure 22. Noise and vibrations of M1 connected to the grid.

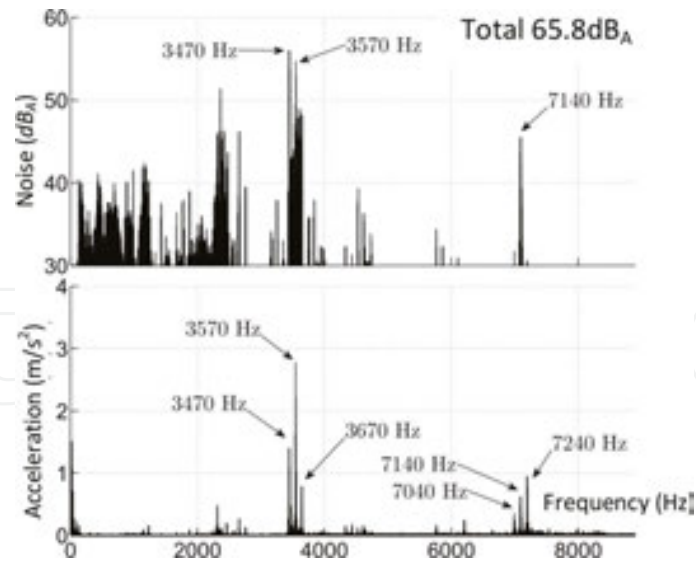


Figure 23. Noise and vibrations of M2 connected to the grid.

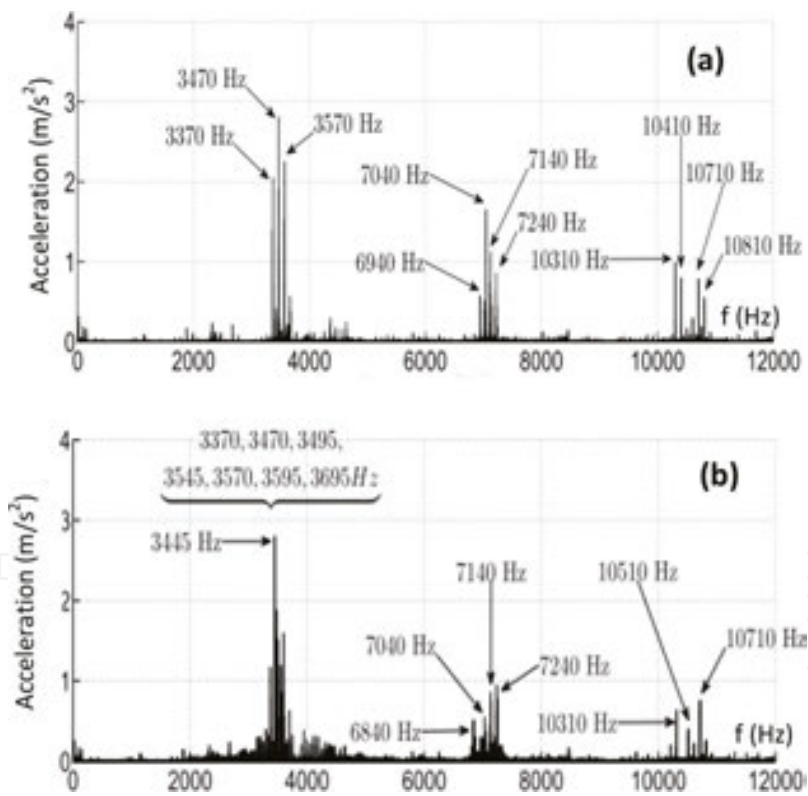


Figure 24. Vibrations of M2:

- (a) connected to a single carrier ( $S\Delta$ ) PWM— $m=70.4$ ,  $r=1$ .
- (b) connected to ( $S\Delta$ ) PWM— $m=70.4$ ,  $r=1$  and carrier phase jump.

Alternative cancellation of  $2m+1$  and  $2m-1$  harmonic ranks.

Since the control techniques must be adapted to the problems that appear on machines taking into account their design, the presented results concern either M1 or M2. Note that these two IMs are not especially sensitive to magnetic noise generated by STPHSs and, therefore, will not lead, in terms of reducing vibrations and noise, to performance that can be described as exceptional. However, the effects are significant enough to validate our developments.

- **Figure 20** shows M<sub>1</sub> equipped with three accelerometers A1, A2, and A3 (A2 and A3 are shifted spatially from 45° to 90° with respect to A1) to, on the one hand, characterize the mode numbers of the Maxwell force components and, on the other hand, to be sure to consider the effects generated by unbalanced STPHSs in accordance with what was presented in section II.3. **Figure 21** gives the results of nodal analysis performed on M<sub>1</sub> that shows that it is particularly sensitive to frequencies around 2800 Hz, 3800 Hz, 4800 Hz, and 6200 Hz.

For the test results to be presented, the IMs are supplied by fundamental 50 Hz three-phase systems with an implementation of a (SΔ) PWM for  $r = 1$ .

- **Figures 22 and 23** show the noise and vibration spectra of, respectively, M1 and M2 directly connected to the grid. In this case, in terms of noise, the mechanical, aerodynamic and magnetic effects appear simultaneously. As can be noted, these “low frequency” effects generate a relatively significant overall noise (66.5 dBA for M1 and 65.8 dBA for M2). The M2 spectra shows more clearly the slotting effect by covering a wider frequency range given the highest values of  $N^s$  and  $N^r$ . In this case, the slotting effect will interfere with the noise components generated by the STPHSs as seen in **Figure 24** where  $m = 70.4$ . Note that specific procedures have been developed to minimize the slotting magnetic noise as presented in reference [30].
- **Figure 24a** shows the M2 acceleration spectra using a conventional (SΔ) PWM inverter that uses only one carrier. Note that the overall noise is 65.8 dBA when M2 is supplied directly by the grid and 66.4 dBA when M2 is supplied via the inverter. As already mentioned, this machine is not particularly sensitive to STPHSs though, from a vibrational point of view, the impact on first and second groups of spectral lines, respectively, centered on 3520 and 7040 Hz is clearly visible.

The carrier-phase jump has been implemented on M2 to reduce the effects of STPHSs centered on  $2m$  eliminating alternatively harmonics of ranks  $2m + 1$  and  $2m - 1$ . To optimize this control, analytical developments show that the constant values must be adjusted as follows:  $C_{(x)} = 0$ ,  $C_{(y)} = 8\pi/3$ . **Figure 24b** shows the impact of this control strategy on the spectral content of vibrations in areas that contain these harmonics. Spread spectrum with reduced amplitudes of the initial components is clearly visible with the appearance of an impact on the third group of components.

- **Figure 25** shows in terms of M1 vibrations, the impact of an adaptation of carrier frequencies with  $m_1 = 39$ ,  $m_2 = 48$ , and  $m_3 = 57$ . Again, the positive impact of this control strategy is clear.

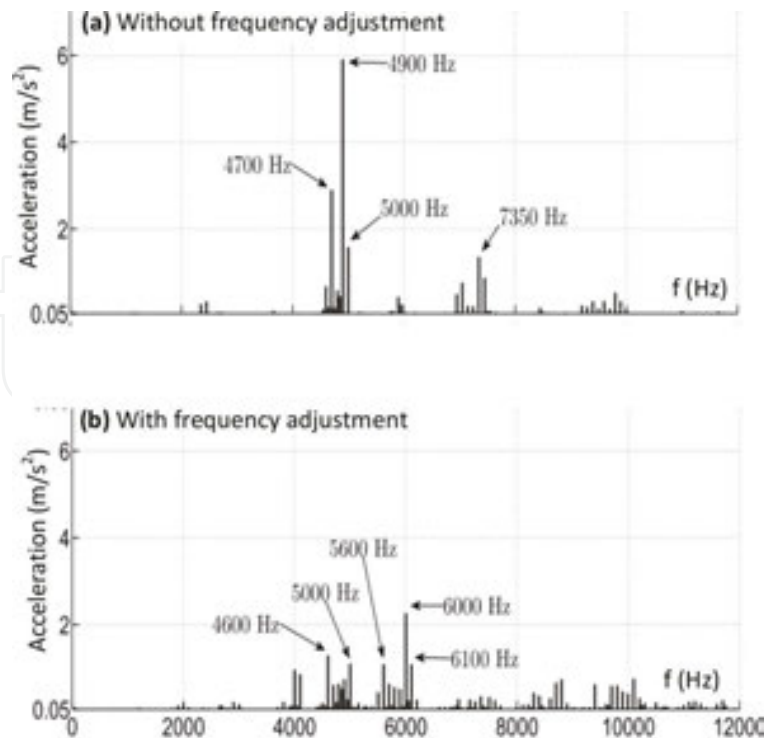


Figure 25. Vibrations of M1—Impact of a carrier frequency shift.

## 8. Conclusion

The proposed calculation method is particularly interesting, because of its implementation simplicity, to characterize the STPHS phase sequences that have a direct impact on the definition of the force components at the origin of the magnetic noise generated by AC machines. On the other hand, it allows anticipating easily over the entire audible frequency range of the spectrum, the consequences of certain control strategies for reducing this noise. Regarding the strategies proposed, they have been analyzed on the basis of experiments on noise and radial vibrations.

## Author details

Jean-François Brudny\*, Fabrice Morganti and Jean-Philippe Lecointe

\*Address all correspondence to: [jfrancois.brudny@univ-artois.fr](mailto:jfrancois.brudny@univ-artois.fr)

Laboratoire Systèmes Electrotechniques et Environnement (LSEE), Univ. Artois, Béthune, France

## References

- [1] Murphy JMD, Turnbull FG. Power electronic control of AC motors, Pergamon Press, New York, 1988.
- [2] Romary R, Brudny JF. Harmonic torques of electrical AC electrical drives. *Industrial Electronics Handbook*. 2nd ed., CRC Press & IEEE Press. Part II, Chapter 11, février 2011. ISBN: 9781439802854, ISBN 10: 1439802858. p. 10.1-10.27.
- [3] Khomfoi S, Kinnares V., Viriya P. Influence of PWM characteristics on the core losses due to harmonic voltages in PWM fed induction motors. In *Proceedings of Power. Eng. Society Winter Meeting*. Publisher IEEE, DOI: 10.1109/PESW2000.849991, Vol. 1, 2000, pp. 365–369.
- [4] Boglietti A, Cavagnino A. Iron loss prediction with PWM supply: An overview of proposed methods from an engineering application point of view. *Electric Power Systems Research* 80, N 9, 2010, pp. 1121–1127.
- [5] Iida S, Okuma Y, Masukawa S, Miyairi S, Bose BK. Study on magnetic noise caused by harmonics in output voltages of PWM inverter. *IEEE Trans. on Industrial Electronics*, 38, N 3, 1991, pp. 180–186.
- [6] Pellerey P, Favennec G, Lanfranchi V, Friedrich G. Active reduction of electrical machines magnetic noise by the control of low frequency current harmonics. In: *Proceedings of IECON 2012—38th Annual Conference on IEEE Industrial Electronics Society*, October 2012, pp. 1654–1659.
- [7] Mihaila V, Duchesne S, Roger D. A simulation method to predict the turn-to-turn voltage spikes in a PWM fed motor winding. *IEEE Trans. on Dielectric and Electrical Insulation*, Vol. 18, N 5, 2011, pp. 1609–1615.
- [8] Cavallini A, Fabiani D, Montanari GC. Power electronics and electrical insulation systems—Part 2: life modeling for insulation design. *DIES, IEEE Electrical Insulation Magazine*, Vol. 26, N 4, 2013, p. 33–39.
- [9] Malinowski M, Gopakumar K, Rodriguez J, Pérez MA. A survey on cascaded multilevel inverters. *IEEE Trans. on Industrial Electronics*, Vol. 57, N° 7, 2010, pp. 2197–2206.
- [10] Le Besnerais J, Lanfranchi V, Hecquet M, Romary R, Brochet P. Optimal slot opening width for magnetic noise reduction in induction motors. *IEEE Trans. on Energy Conversion* 2009, Vol. 24, N 4, pp. 869–874.
- [11] Brudny JF, Lecoite JP. Rotor design for reducing the switching magnetic noise of AC electrical machine variable-speed drives. *IEEE Trans. on Industrial Electronics*, Vol. 58, 2011, p. 5112–5120.
- [12] Madarres M, Vahedi A, Ghazanchaei MR. Investigations on dynamic and steady state performance of axial flux hysteresis motors considering rotor configurations.

International Review of Electrical Engineering, Vol. 5, N 1, ISSN 1827-6660, 2010. p. 105.

- [13] Da Silva ERC, Dos Santos EC, Jacobina CB. Pulsewidth modulation strategies. IEEE Ind. Electr. Mag, 5, 2, 2011, pp. 37–45.
- [14] Kim DJ, Jung JW, Hong JP, Kim KJ, Park CJ. A study on the design process of noise reduction in induction motors. IEEE Trans. on Magnetics, Vol. 48, N 11, 2012, pp. 4638–4641.
- [15] Habetler TG, Divan DM. Acoustic noise reduction in sinusoidal PWM drives using a randomly modulated carrier. IEEE Trans. Power Electr., Vol. 6, 1991, pp. 356–363.
- [16] GA Covic, Boys JT. Noise quieting with random PWM AC drives. IEE Proc. Electr. Power Appl, Vol. 145, N1, January 1998, pp. 1–10.
- [17] Le Besnerais J, Lanfranchi V, Hecquet M, Brochet P. Characterization and reduction of audible magnetic noise due to pwm supply in induction machines. IEEE Trans. Ind. Electr., Vol. 57, N 4, 2010, pp. 1288–1295.
- [18] Ruiz-Gonzalez A, Meco-Gutierrez MJ, Perez-Hidalgo F, Vargas-Merino F, Heredia-Larrubia JR. Reducing acoustic noise radiated by inverter-fed induction motors controlled by a new PWM strategy. IEEE Trans. Ind. Electr., Vol. 57, N 1, 2010, pp. 228–236.
- [19] Tischmacher H, Eichinger B. Sound optimisation of a converter-fed drive system using an acoustic camera in combination with modal analysis, COMPEL Vol. 29, N 4, 2010, p. 908.
- [20] Szkudlanski T, Lecointe JP, Morganti F, Brudny JF. AC rotating machine radial vibrations: a principle to reduce the PWM switching effects. Proceedings of International Symposium on Electromagnetic Field, ISEF, Ohrid, Macedonian September 2013, PS5–271.
- [21] Brudny JF, Szkudlanski T, Morganti F, Lecointe JP. Method for controlling the PWM switching: application to magnetic noise reduction. IEEE Trans. Ind. Electr., Vol. 62, N 1, 2015, pp. 122–131.
- [22] Brudny JF, Morganti F, Lecointe JP, Parent G. On the use of carrier phase jumps to reduce some PWM switching effects. In Proceedings of IECON 2014—40th Annual Conf. on IEEE Industrial Electronics Society, Dallas, Texas, USA, October 2014, pp. 762–768.
- [23] Alger PL. The nature of induction machines. 2nd ed, Gordon and Breach Publishers, New-York, London, Paris, 1970.
- [24] Timar PL, Fazekas A, Kiss J, Miklos A, Yang SJ. Noise and vibration of electrical machines. Elsevier Amsterdam, Oxford, New York, Tokyo, 1989.
- [25] Brudny JF. Modelling of induction machine slotting. Resonance phenomenon. European Physical Journal, Applied Physic, JP III, 1997, pp. 1009–1023.

- [26] Lecointe JP, Romary R, Brudny JF, Czaplá T. Five methods of stator natural frequency determination: case of induction and switched reluctance machines. *Mechanical Systems and Signal Processing*, MSSP, Academic Press, Cambridge, UK. 2004, pp. 1133–1159.
- [27] Bowes SR. New sinusoidal pulse width-modulated inverter. *Proceedings of the Institution of Electrical Engineers*, Vol. 122, N 11, 1975, pp. 1279–1285.
- [28] Holmes DG. A general analytical method for determining the theoretical harmonic components of carrier based PWM strategies. *Proceedings of Thirty-Third IAS Annual Meeting*, St Louis, MO, USA, IEEE Publisher, Vol. 2, October 1998, pp. 1207–1214.
- [29] Sun J, Grotstollen H. Fast time-domain simulation by waveform relaxation methods, *IEEE Trans. on Circuits and Systems I: Fundamental Theory and Applications*, Vol. 44, N 8, 1997, pp. 660–666.
- [30] Cassoret B, Corton R, Roger D, Brudny JF. Magnetic noise reduction of induction machines. *IEEE Trans. on Power Electronics*, Vol. 18, N 2, 2003, pp. 570–579.